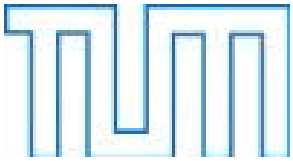

Fakultät für Medizin der Technischen Universität München
II. Medizinische Klinik und Poliklinik

Kinase Recomplementation Screen in Pdk1-deleted Pancreatic Tumour Cell Lines

Lucia Giovanna Maria Liotta

Vollständiger Abdruck der von der Fakultät für Medizin der Technischen Universität München zur Erlangung des akademischen Grades eines
Doktors der Medizin
genehmigten Dissertation.

Vorsitzender: Prof. Dr. Jürgen Schlegel

Prüfer der Dissertation:
1. Prof. Dr. Dieter Saur
2. Priv.-Doz. Dr. Anna M. Schlitter

Die Dissertation wurde am 28.11.2019 bei der Technischen Universität München eingereicht und durch die Fakultät für Medizin am 11.08.2020 angenommen.

Acknowledgements

I would like to thank Prof. Dr. Dieter Saur for letting me work in his research group and for his guidance.
I would also like to thank Prof. Dr. Roland Schmid for giving me the opportunity to work at the II. Medizinische Klinik at Klinikum rechts der Isar.
Moreover, I am very grateful to Dr. Christian Veltkamp for his valuable teachings, supervision of my work and revision of the thesis.
Special thanks to all members of Saur/Schneider lab, especially to Christian Schneeweis, Magdalena Zukowska, Barbara Seidler, Zonera Hassan, Vanessa Schöllhorn and Dorothea Höpfner for their technical help, the stimulating discussions and their contribution to my project.
Finally, I thank my family and my fiancé for their moral support.

Inhaltsverzeichnis

List of tables

List of figures

Abbreviations

°C	degree Celsius
4-OHT	tamoxifen
A	adenine
ADM	acinar-to-ductal metaplasia
APS	ammonium persulfate
BMI	body mass index
bp	base pairs
BSA	bovine serum albumin
C	cytosine
CDK	cyclin-dependent kinase
cDNA	complementary deoxyribonucleic acid
CypA	cyclophilin
D-MEM	Dulbecco's modified eagle medium
DMSO	dimethylsulfoxide
DNA	deoxyribonucleic acid
EMT	epithelial-mesenchymal transition
ER	estrogen receptor
Erk	mitogen-activated protein kinase kinase kinase 1
EtOH	Ethanol
FCS	fetal calf serum
g	gram
G	guanine
GEM	genetically engineered mouse model
GSK3β	glycogen synthase kinase 3 beta
GTP	guanosine triphosphate
h	hours
HEK	human embryonic kidney
IPMN	intraductal papillary mucinous neoplasm
kb	kilobase pairs
kDa	kilodalton
KO	knock-out
LSL	loxP-stop-loxP
M	mol / molar
MAPK	mitogen-activated protein kinase
mg	milligram
min	minutes
mL	milliliter
mm	millimeter

mM	millimol / millimolar
mut	mutated
NES	nuclear export signal
ng	nanogram
nm	nanometer
nM	nanomol / nanomolar
p	phospho
PanIN	pancreatic intraepithelial neoplasia
PBS	phosphate buffered saline
PCR	polymerase chain reaction
PDAC	pancreatic ductal adenocarcinoma
Pdx1	pancreatic and duodenal homeobox 1
PI3K	phosphoinositide 3-kinase
PTEN	phosphatase and tensin homolog
Ptf1a	pancreas transcription factor subunit alpha
pWZL	Vector backbone
R26	Rosa26
Rb	retinoblastoma
RNA	ribonucleic acid
Rpm	rounds per minute
RT	room temperature
SDS	sodium dodecyl sulfate
sec	seconds
T	thymine
TAE	tris acetate EDTA
TBS	tris buffered saline
TEMED	N,N,N',N'-tetramethylethylenediamine, 1,2-bis(dimethylamino)-ethane
TGFβ	transforming growth factor β
TP53/Trp53	transformation related protein 53
U	units
V	volt
wt	wild type
µg	microgram
µL	microliter
µm	micrometer
µM	micromol / micromolar

1 Abstract

Previous studies have shown that the PI3K effector Pdk1 is essential for the initiation of pancreatic ductal adenocarcinoma (PDAC) and its loss leads to complete blockage of acinar-to-ductal-metaplasia (ADM), pancreatic intraepithelial neoplasia (PanIN) and PDAC formation in the *Kras*^{G12D}-driven PDAC model.

Pdk1 is important for the growth of *Kras*^{G12D}-driven pancreatic tumour cell lines, since *Pdk1*-knock-out (KO) cells show a significantly decreased growth and a reduction in the metabolic activity.

Up to now, it has not been understood which Pdk1-dependent signalling pathways are involved in PDAC progression as well as how resistance mechanisms against PI3K/PDK1 inhibition develop.

For this reason, I examined which kinases are able to rescue the loss of Pdk1 in *Kras*^{G12D}-driven PDAC cells which are derived from genetically engineered mouse models (GEMMs) hosting an inducible dual recombinase system, where a tamoxifen treatment leads to a *Pdk1*-KO.

By expressing almost thirty myristoylated, and thus constitutively active, kinases, both Pdk1 direct targets and Pdk1-independent kinases were analysed, in order to see which kinases are able to compensate the loss of Pdk1.

The expression of myristoylated Akt1, one of the main direct targets of Pdk1, led to a complete rescue of Pdk1 loss both in MTT and clonogenic assay.

A partial rescue of Pdk1 loss was obtained by expressing CKS1B-myr, RSK3-myr and RPS6KA5-myr. CKS1B is often amplified in human PDAC and so far not been associated with PI3K signaling.

Considering that no therapy addressing KRAS or PI3K has been successful so far, this study could help to better understand the mechanisms of resistance in PDAC.

2 Zusammenfassung

Kürzlich konnte gezeigt werden, dass Pdk1, ein PI3K Effektor, einen wichtigen Effektor der Genese des Pankreaskarzinoms darstellt.

Im *Kras*^{G12D}-getriebenen Pankreaskarzinommodel verhindert sein Verlust die Entwicklung von ADM, PanIN und PDAC.

Pdk1 ist für das Wachstum von *Kras*^{G12D}-getriebenen Pankreastumorzelllinien notwendig, da *Pdk1*-KO zur deutlichen Wachstumsreduktion sowie Verlangsamung der metabolischen Prozesse führt.

Bisher sind allerdings die genauen Pdk1-abhängigen Signalkaskaden in der PDAC-Progression sowie die Resistenzmechanismen gegen die Pi3k/PDK1 Inhibition noch unklar.

Aus diesem Grund habe ich in dieser Arbeit untersucht, welche Kinasen verantwortlich sind für die Rettung vom Pdk1 Verlust in *Kras*^{G12D}-getriebenen Pankreastumorzelllinien aus genetisch veränderten Mausmodellen, wo *Kras*^{G12D} nur im Pankreas konstitutiv aktiviert und *Pdk1* durch eine Behandlung mit Tamoxifen deletiert wird.

Durch die Überexpression von fast dreißig myristoylierten und dadurch konstitutiv aktiven Kinasen, wurde untersucht welche direkten Effektoren von Pdk1 und welche Pdk1-unabhängige Kinasen den Verlust von Pdk1 ersetzen können.

Die Überexpression von myr-Akt1, einer der wichtigsten Pdk1-Effektoren, konnte seinen Verlust vollständig retten.

Die Überexpression von CKS1B, RSK3 und RPS6KA5 konnten zudem den Pdk1-Verlust zum Teil retten. CKS1B ist oft im humanen PDAC amplifiziert aber bislang nicht assoziiert mit der PI3K Signalkaskade.

Zusammengefasst, deuten meine Ergebnisse darauf hin, dass diese Kinasen eine Rolle als Pdk1 Effektoren spielen und ein besseres Verständnis der Tumorresistenzmechanismen ermöglichen können.

3 Introduction

3.1 Pancreatic Cancer

Pancreatic cancer is a life-threatening disease, leading to death despite treatment in almost 95% of the patients within 5 years (Ma and Jemal, 2013).

A recent epidemiological study showed that pancreatic cancer was the fourth most fatal cancer in men and women (Malvezzi et al., 2014). In contrast to the other most frequent malignancies, pancreatic cancer did not show an improvement in terms of life expectancy (Malvezzi et al., 2014).

Pancreatic tumours are generally malign (98%) and could arise both from the exocrine (95%) or the endocrine (mainly neuroendocrine tumours) parts of the pancreas.

Histologically, the vast majority (90%) of pancreatic carcinomas are adenocarcinomas arising from the ductal epithelial cells (PDAC) (Bryant et al., 2014). Other less frequent types of pancreatic cancer are adenosquamous carcinoma, undifferentiated carcinomas with osteoclast-like giant cells and acinar cell pancreatic cancer (Rishi et al., 2015).

About 5-10% of pancreatic cancers are related to germline genetic alterations. Most familial pancreatic cancer cases are associated with *BRCA1* or *BRCA2* mutations (Iqbal et al., 2012). Other familial syndroms are Li-Fraumeni Syndrome (Amadou et al., 2018), hereditary pancreatitis (Langner, 2017), hereditary non-polyposis colorectal cancer (Gargiulo et al., 2009, Kastrinos et al., 2009), hereditary breast and ovarian cancers (Matsubayashi et al., 2017), Peutz–Jeghers syndrome (Giardiello et al., 2000, Rebours et al., 2008), ataxia telangiectasia (Roberts et al., 2012) and familial atypical multiple mole melanoma syndrome (Ducreux et al., 2015). The major known environmental risk factors are tobacco (Bosetti et al., 2012, Lowenfels and Maisonneuve, 2004), *Helicobacter pylori* infection (Hirabayashi et al., 2019) and factors related to dietary habits (BMI, red meat intake, low fruit and vegetable intake, diabetes, alcohol intake) (Ducreux et al., 2015).

The only potentially curative therapy for PDAC is the complete surgical resection (Hidalgo, 2010). Unfortunately, this can only happen when the malignancy is diagnosed at an early stage and is generally only considered when distant metastases are not detected. Therefore, only about 20% of all patients with PDAC are diagnosed at a stage where tumour resection is taken into account with a curative intention (Ducreux et al., 2015).

The 5-year survival after surgery is about ~20% (Ducreux et al., 2015). Patients with a non resectable or metastasized tumour are treated with a palliative therapy mainly based on gemcitabine (with or without nab-paclitaxel) or FOLFIRINOX regimen (Ducreux et al., 2015).

The main reasons for the poor prognosis are related to the fact that pancreatic cancer is generally highly aggressive and that it typically leads to symptoms when it is already advanced. Moreover, pancreatic cancer is often resistant to the conventional radio and chemotherapy (Lemke et al., 2014).

3.2 Progression of pancreatic cancer

The most frequent PDAC precursors are microscopic pancreatic intraepithelial neoplasia (PanIN), less frequently IPMN and mucinous cystic neoplasm (Ducreux et al., 2015). The most common progression model is based on PanIN lesions divided into 1A, 1B, 2 and 3 leading to invasive PDAC (Hruban et al., 2000). As a new precursor for PDAC, a process known as acinar-to-ductal-metaplasia (ADM) has recently been identified. This process precedes PanIN formation and is a characteristic of chronic pancreatitis (Pinho et al., 2011).

Moreover, it has recently been suggested that atypical flat lesions originating in areas of ADM could be a probable precursors of PDAC and similar lesions were also found in the pancreas of some patients with a family history of PDAC (Aichler et al., 2012).

However, a new tumourigenesis model for pancreatic cancer has recently been suggested by Notta and colleagues according to which chromothripsis, which consists in thousands of chromosomal rearrangements occurring altogether in specific unstable genomic regions, is presented as an alternative route for pancreatic cancer to obtain an aggressive behavior (Notta et al., 2016).

3.3 Role of *KRAS* in PDAC

Mutant KRAS is mostly associated with PDAC's initiation and development and the consitutive activation of KRAS leads to ADM, PanIN, invasive PDAC and metastasis (Collins et al., 2012a, Collins et al., 2012b)

It has been demonstrated that KRAS is mutated in about almost 100% of Pan-IN lesions and invasive PDACs (Hruban et al., 2008) . These data support the idea that KRAS is very important in all stages of development of pancreatic cancer.

Besides stimulating cell proliferation, oncogenic KRAS is also responsible for evasion of apoptosis, alterations in metabolism, evasion of the immune system response and microenvironmental changes in PDAC, by enhancing inflammation and desmoplasia (Eser et al., 2014, Pylayeva-Gupta et al., 2011).

KRAS belongs to *RAS* family, which also includes *HRAS* and *NRAS* (di Magliano and Logsdon, 2013), coding for 21 kDa proteins. About 98% of the *KRAS* mutations in PDAC occur at codon 12 leading to the substitution of a glycin (G) with aspartic acid (D) residue (Eser et al., 2014). Subsequently, the intrinsic rate of GTP hydrolysis is inhibited leading to constitutive activation of KRAS downstream pathways (Scheffzek et al., 1997).

KRAS activates several effector pathways (RAF-MEK-ERK, PI3K/AKT, RalGDS/p38MAPK, Rac and Rho, Rassf1, NF1, p120GAP and PLC-ε) (Castellano and Downward, 2011, di Magliano and Logsdon, 2013).

Progression of PDAC requires inactivation of tumour suppressors like *CDKN2A* encoding for $p16^{INK4A}$, $p14^{ARF}$, *TP53* and *SMAD4* (Bryant et al., 2014). Since the attempts to directly target Kras failed so far (Berndt et al., 2011), it is necessary to develop new therapies based on its downstream pathways.

3.4 Raf/Mek/Erk and PI3K/Akt Pathway

The RAF/ERK/MEK pathway is the canonical KRAS pathway. KRAS binds to RAF and thus activates it (Collisson et al., 2012). Once RAF is activated by KRAS, MEK1 and MEK2 are phosphorylated. MEK is a mitogen-activated protein kinase kinase (MAPKK) that activates ERK, a mitogen-activated protein kinase (MAPK). ERK 1/2 have several substrates, among which are several members of the RSK family (Yoon and Seger, 2006).

The PI3K pathway is important in PDAC progression and maintainance and PI3K inhibitors prevent tumour progression in $Kras^{G12D}$-dependent mouse models and humanized xenotransplantation models of PDAC (Schneider et al., 2007).

The PI3K/AKT pathway is activated both in human and murine PDAC and leads to the activation of PDK1. PI3K is encoded by *PI3KCA*.

The *Pik3ca*^{H1047R} mutation in a *Ptf1a*$^{Cre/+}$-based mouse model shows similar ADM induction and PanIN progression to *Ptf1*$^{Cre/+;}$*LSL-Kras*$^{G12D/+}$ mutated mice models.
Since the Cre recombinase is expressed under the control of the *Ptf1a* promoter, it is specifically expressed in pancreatic precursor cells.
Pi3k signaling induces ADM, PanIN and PDAC formation and is activated during the first stages of PDAC development.
There are three major *PIK3CA* mutations (E542K, E545K and H1047R) that lead to downstream activation of Pdk1 or AKT in the tumour development (Wu et al., 2014).
PI3K is a heterodimeric kinase which consists of two subunits: p110a and p85. The former is the catalytic subunit and the latter the regulatory one. Once bound to a tyrosine kinase receptor, p85 removes the inhibitory effect on p110 and PI3K becomes active. PI3K phosphorylates PIP2 to PIP3, which recruits Pdk1 to the cell membrane and activates it. Pdk1 is constitutively active in the cell due to its ability to phosphorylate its own T-loop (Hofler et al., 2011). Pdk1 is a member of the AGC (cAMP-dependent protein kinases A, cGMP-dependent protein kinases G, and phospholipid-dependent protein kinases G) kinase family and, once activated, phosphorylates several proteins (e.g. AKT, p70s6k, SGK, RSK, PKC, PKN1). Pdk1 is able to perform a trans-autophosphorylation of its activation segment residue (Ser241) (Pearce et al., 2010). Thus, it is consitutively active.
Pdk1 is essential for PDAC initiation and its loss leads to complete blocking of ADM, PanIN and PDAC formation in the Kras^{G12D} model.
AKT is one of the main direct targets of Pdk1. The formation of PIP3 triggers membrane-based colocalization of Pdk1 and AKT, which bind to PIP3 through their pleckstrin homology (PH) domains (Hofler et al., 2011). AKT is then recruited to the plasma membrane and it changes its conformation. Consequently, it can be phosphorylated by Pdk1 on the T308 residue (Majumder and Sellers, 2005). This leads to its partial activation, but, in order to gain the complete activation, AKT needs to be phosphorylated by mTORC2 (mammalian target of rapamycin complex 2) and other kinases on a Ser473 and Thr 450 residue (Hofler et al., 2011). The PI3K/AKT pathway is counteracted by the tumour suppressor PTEN (phosphatase and tensin homolog deleted on chromosome 10) through the dephosphorylation of PIP3 (Hofler et al., 2011). The PI3K/AKT signaling pathway was shown to be constitutively activated due to an aberrant expression of PTEN in pancreatic cancer cells (Asano et al., 2004).

AKT belongs to the AGC kinase family and there are three different isoforms: AKT1, AKT2, AKT3. AKT1 and 2 are known to be involved in several tumour types: AKT1 mainly in colorectal and gastric cancer; AKT2 in breast and ovarian cancer (Hofler et al., 2011).

AKT stimulates tumourigenesis by phosphorylating, and thus activating, substrates involved in cell cycle progression and inactivating others involved in apoptosis (BAD, FASL). Other targets involved in cell growth are FOXO and HDM2. AKT plays a role also in glucose metabolism (Pearce et al., 2010).

For example, the activation of Akt leads to an increase in the expression of the glucose transport Glut1 in the cells (Barthel et al., 1999, Wieman et al., 2007, Elstrom et al., 2004), mediates the response of Glut1 gene to insulin and promotes the cell trafficking of Glut1 (Wieman et al., 2007). Moreover, Akt is regarded as the most important signal transducer of insulin in both liver and glucose transporter type 4–dependent tissues. In fact the constitutively active Akt induces glucose uptake into adipocyte by stimulating the translocation of the insulin-responsive glucose transporter 4 (Glut4) to the plasma membrane, even without insulin stimulation (Kohn et al., 1996).

It was shown that overexpression of constitutively active Akt in the mouse liver results in hypoglycemia (Ono et al., 2003) and that its activation suppresses hepatic gluconeogenesis (Wang et al., 2012) while deletions of hepatic Akt1 and Akt2 induce hyperglycemia and insulin resistance (Lu et al., 2012).

3.5 Generation of *Pdx1-Flp; FSF-Kras$^{G12D/+}$; FSF-R26$^{CAG-CreERT2/+}$; Pdk1$^{lox/lox}$* cell line

The cell lines used in this study were derived from genetically engineered mouse models (GEMMs) with a dual recombinase system (Schonhuber et al., 2014), which combines the Flippase-FRT (*Flp*-FRT) and *Cre*-loxP recombination technologies. The FSF (Frt-Stop-Frt) cassette can be deleted by a Cre or Flp recombinase associated with a tissue specific promoter, in order to manipulate the gene expression. Flp expression is driven by the murine, pancreas-specific Pdx1 promoter. This enables the constitutive expression of an FSF silenced oncogenic Kras^{G12D} (FSF- Kras$^{G12D/+}$) only in the pancreas, which causes metastatic PDAC.

The *Flp*-recombined cells are manipulated through a tamoxifen-inducible allele (Cre-ERT2) silenced by an FSF cassette controlled by the CAG promoter as a knock-in in the Rosa26 locus (*FSF-R26$^{CAG-CreERT2/+}$).* In our GEMMs tamoxifen treatment induces the translocation of Cre, which removes a *lox*P-flanked transcriptional and translational stop element of the exone 3 and 4 of the *Pdk1* locus, leading to a pancreas specific *Pdk1*-KO. Previous experiments have shown that growth of *Pdk1$^{lox/lox}$;LSL-Trp53$^{R172H/+}$* cell lines is not affected by treatment with tamoxifen.

The cells used in this study are mainly *Pdk1$^{lox/lox}$;LSL-Trp53$^{R172H/+}$* cell lines. In order to validate the results of the overexpression of Akt1, RPS6KA5 and CKS1B, the other cell lines used are *Pdk1$^{lox/lox}$;Trp53$^{frt/+}$* cells.

After deletion of the LSL cassette by Cre recombinase, oncogenic *Trp53$^{R172H/+}$* is expressed. Previous experiments have shown that *Pdk1$^{lox/lox}$;*Trp53$^{R172H/+}$ cells without CreER^{T2} grew normally after 4-OHT treatment and thus validating that the Pdk1 deletion and not the *Trp53$^{R172H/+}$* expression is responsible for the observed effects in Pdk1-KO cells. If not specified, the cells used in this study are *Pdk1$^{lox/lox}$;*Trp53$^{R172H/+}$ cells.

4 Aim

Pdk1 is essential for the initiation of *Kras*^{G12D}-driven PDAC (Schonhuber et al., 2014). Furthermore, several experiments show that the loss of Pdk1 in the dual recombinase system leads to a reduced tumour growth and impaired metabolic activity indicating an important function in tumour maintainance as well.

The main aim of this research project is to find out which kinases can compensate the loss of Pdk1. Both Pdk1 direct targets and independent kinases will be analysed, in order to see whether they are able to rescue the loss of Pdk1.

This will be achieved by expressing myristoylated kinases in *Kras*^{G12D} driven *Pdk1*$^{lox/lox}$ pancreatic tumour murine cell lines.

5 Materials

5.1 Devices

Table 1. Devices

Device	Source
96-well magnetic ring-stand	Applied Biosystems, Inc., Carlsbad, CA, USA
Autoclave 2540 EL	Tuttnauer Europe B.V., Breda, The Netherlands
Bag sealer Folio FS 3602	Severin Elektroger.te GmbH, Sundern
Centrifuge Avanti. J25	Beckman Coulter GmbH, Krefeld
Centrifuge Rotina 46R	Andreas Hettich GmbH & Co. KG, Tuttlingen
CO2 incubator HERAcell.	Heraeus Holding GmbH, Hanau
CO2 incubator MCO-5AC 17AI	Sanyo Sales & Marketing Europe GmbH, Munich
Dewar carrying flask, type B	KGW-Isotherm, Karlsruhe
Duo therm hybridization oven OV5	Biometra GmbH, Goettingen
Electrophoresis power supply Power Pac 200	Bio-Rad Laboratories GmbH, Munich
Electroporation system Gene Pulser. II	Bio-Rad Laboratories GmbH, Munich
Experion. automated electrophoresis station	Bio-Rad Laboratories GmbH, Munich
Experion. priming station	Bio-Rad Laboratories GmbH, Munich
Experion. vortex station	Bio-Rad Laboratories GmbH, Munich
Gel Doc™ XR+ system	Bio-Rad Laboratories GmbH, Munich
Glass ware	Schott Duran. Schott AG, Mainz
HERAsafe. biological safety cabinet	Thermo Fisher Scientific, Inc., Waltham, MA, USA
Horizontal gel electrophoresis system	Biozym Scientific GmbH, Hessisch Oldenburg
Horizontal shaker	Titertek Instruments, Inc., Huntsville, AL, USA
Incubator shaker Thermoshake	C. Gerhardt GmbH & Co. KG, K.nigswinter
Laminar flow HERAsafe	Heraeus Holding GmbH, Hanau
Liquid scintillation counter & luminometer	PerkinElmer, Rodgau
Magnetic stirrer, Ikamag. RCT	Wallac 1450 MicroBeta TriLux
Microcentrifuge 5415 D	IKA. Werke GmbH & Co. KG, Staufen
Microcentrifuge 5417 R	Eppendorf AG, Hamburg
Microplate reader Anthos 2001	Eppendorf AG, Hamburg
Microscope Axio Imager.A1	Anthos Mikrosysteme GmbH, Krefeld
Microscope Axiovert 25	Carl Zeiss AG, Oberkochen
Microscope DM LB	Carl Zeiss AG, Oberkochen
Microwave	Leica Microsystems GmbH, Wetzlar
Mini centrifuge MCF-2360	Siemens, Munich

Mini-PROTEAN. Tetra Cell	LMS Consult GmbH & Co. KG, Brigachtal
Multipette. stream	Bio-Rad Laboratories GmbH, Munich
Odyssey. infrared imaging system	Eppendorf AG, Hamburg
pH meter 521 WTW	Li-Cor Biosciences, Lincoln, NE, USA
Pipettes Reference.	Wissenschaftlich-Technische Werkstätten GmbH,Weilheim
Pipetus	Eppendorf AG, Hamburg
Power supplies E844, E822, EV243	Hirschmann Laborger.te GmbH & Co. KG,Eberstadt
Spectrophotometer NanoDrop 1000	Peqlab Biotechnologie GmbH, Erlangen
StepOnePlus™ real time PCR system	Peqlab Biotechnologie GmbH, Erlangen
Thermocycler T1	Applied Biosystems, Inc., Carlsbad, CA, USA
Thermocycler TGradient	Biometra GmbH, Goettingen
Thermocycler TPersonal	Biometra GmbH, Goettingen
Thermocycler UNO-Thermoblock	Biometra GmbH, Goettingen
Thermomixer compact	Biometra GmbH, Goettingen
Vortex Genius 3	Eppendorf AG, Hamburg
Water bath 1003	IKA. Werke GmbH & Co. KG, Staufen
Western blot system SE 260 Mighty Small II	GFL Gesellschaft für Labortechnik mbH, Burgwedel

5.2 Disposables

Table 2. Disposables

Disposable	Source
Cell culture plastics	Becton Dickinson GmbH, Franklin Lakes, NJ, USA; Greiner Bio-One GmbH, Frickenhausen; TPP Techno Plastic Products AG, Trasadingen, Switzerland
Cell scrapers	TPP Techno Plastic Products AG, Trasadingen, Switzerland
Cell strainer, 100 µm, yellow	BD Biosciences, Franklin Lakes, NJ, USA
Chromatography paper, 3 mm	GE Healthcare Europe GmbH, Munich
Combitips BioPur®	Eppendorf AG, Hamburg
Conical tubes, 15 mL	TPP Techno Plastic Products AG, Trasadingen, Switzerland
Conical tubes, 50 mL	Sarstedt AG & Co., Nümbrecht
Cover slips	Gerhard Menzel, Glasbearbeitungswerk GmbH & Co. KG, Braunschweig

CryoPure tubes	Sarstedt AG & Co., Nümbrecht
Cuvettes	Greiner Bio-One GmbH, Frickenhausen
Disposable scalpels	Feather Safety Razor Co., Ltd., Osaka, Japan
Filtropur S 0.2	Sarstedt AG & Co., Nümbrecht
Filtropur S 0.45	Sarstedt AG & Co., Nümbrecht
Glass slides Superfrost® Plus	Gerhard Menzel, Glasbearbeitungswerk GmbH & Co. KG, Braunschweig
MicroAmp® optical 96-well reaction plate	Applied Biosystems, Inc., Carlsbad, CA, USA
Microtome blades S35 and C35	Feather Safety Razor Co., Ltd., Osaka, Japan
Pasteur pipettes	Hirschmann Laborgeräte GmbH & Co. KG, Eberstadt
PCR reaction tubes	Brand GmbH + Co. KG, Wertheim; Eppendorf AG, Hamburg
Petri dishes	Sarstedt AG & Co., Nümbrecht
Pipette tips	Sarstedt AG & Co., Nümbrecht
Reaction tubes, 0.5 mL, 1.5 mL and 2 mL	Eppendorf AG, Hamburg
Safe seal pipette tips, professional	Biozym Scientific GmbH, Hessisch Oldenburg
Safe-lock reaction tubes BioPur®	Eppendorf AG, Hamburg
Serological pipettes	Sarstedt AG & Co., Nümbrecht
Single use needles Sterican® 27 gauge	B. Braun Melsungen AG, Melsungen
Single use syringes Omnifix®	B. Braun Melsungen AG, Melsungen

5.3 Reagents and enyzmes

Table 3. Reagents and enzymes

Reagents and enzymes	Source
1 kb DNA extension ladder	Invitrogen GmbH, Karlsruhe
1,4-Dithiothreitol (DTT)	Carl Roth GmbH + Co. KG, Karlsruhe
2-Log DNA ladder (0.1–10.0 kb)	New England Biolabs GmbH, Frankfurt am Main
2-Mercaptoethanol, 98%	Sigma-Aldrich Chemie GmbH, Munich
2-Propanol (isopropanol)	Carl Roth GmbH + Co.
Agarose	Sigma-Aldrich Chemie GmbH, Munich
Ammonium persulfate	Sigma-Aldrich Chemie GmbH, Munich
Ampicillin sodium salt	Carl Roth GmbH + Co. KG, Karlsruhe
Blotting grade blocker non-fat dry milk	Bio-Rad Laboratories GmbH, Munich
Bovine serum albumin, fraction V	Sigma-Aldrich Chemie GmbH, Munich
Bradford reagent	Serva Electrophoresis GmbH,Heidelberg

Bromphenol blue	Sigma-Aldrich Chemie GmbH, Munich
Complete, EDTA-free, protease inhibitor cocktail, Tablets	Roche Deutschland Holding GmbH, GrenzachWyhlen
Dimethylsulfoxide (DMSO)	Carl Roth GmbH + Co. KG, Karlsruhe
dNTP mix, 10mM each	Fermentas GmbH, St. Leon-Rot
Dodecylsulfate Na-salt in pellets (SDS)	Serva Electrophoresis GmbH, Heidelberg
Dulbecco's phosphate buffered saline, powder	Biochrom AG, Berlin
Ethanol (100%)	Merck KGaA, Darmstadt
Ethidium bromide	Sigma-Aldrich Chemie GmbH, Munich
Ethylenediaminetetraacetic acid (EDTA)	Invitrogen GmbH, Karlsruhe
Gel loading dye, blue	New England Biolabs GmbH, Frankfurt am Main
GeneRuler™ 100bp DNA ladder	Fermentas GmbH, St. Leon-Rot
Glycerol	Sigma-Aldrich Chemie GmbH, Munich
Glycin Pufferan®	Carl Roth GmbH + Co. KG, Karlsruhe
HEPES Pufferan®	Carl Roth GmbH + Co. KG, Karlsruhe
HotStarTaq DNA polymerase	Qiagen GmbH, Hilden
Hydrochloric acid (HCl)	Merck KGaA, Darmstadt
Isotonic sodium chloride solution	Braun Melsungen AG, Melsungen
LB agar (Luria/Miller)	Carl Roth GmbH + Co. KG, Karlsruhe
LB broth (Luria/Miller	Carl Roth GmbH + Co. KG, Karlsruhe
Magnesium chloride	Carl Roth GmbH + Co. KG, Karlsruhe
Methanol	Merck KGaA, Darmstadt
Phosphatase inhibitor mix I	Serva Electrophoresis GmbH, Heidelberg
Polyethylene glycol 4000	Merck KGaA, Darmstadt
Precision Plus Protein™ all blue standard	Bio-Rad Laboratories GmbH, Munich
Proteinase K, recombinant, PCR grade	Roche Deutschland Holding GmbH, Grenzach-Wyhlen
QuantiFast® SYBR® green PCR master mix	Qiagen GmbH, Hilden
REDTaq® ReadyMix™ PCR reaction mix	Sigma-Aldrich Chemie GmbH, Munich
RNase-free DNase set	Qiagen GmbH, Hilden
RnaseA	Fermentas GmbH, St. Leon-Rot
Rotiphorese® gel 30	Carl Roth GmbH + Co. KG, Karlsruhe
Sodium acetate buffer solution	Sigma-Aldrich Chemie GmbH, Munich
Sodium chloride (NaCl)	Merck KGaA, Darmstadt
Sodium hydroxide solution (NaOH)	Merck KGaA, Darmstadt
Tamoxifen	Sigma-Aldrich Chemie GmbH, Munich
TaqMan® reverse transcription reagents	Applied Biosystems, Inc., Carlsbad, CA, USA
TE buffer, pH 8.0	AppliChem GmbH, Darmstadt
TEMED	Carl Roth GmbH + Co. KG, Karlsruhe

Tris hydrochloride	J.T.Baker® Chemicals, Phillipsburg, NJ, USA
Tris Pufferan®	Carl Roth GmbH + Co. KG, Karlsruhe
Triton® X-100	Merck KGaA, Darmstadt
Tween® 20	Carl Roth GmbH + Co. KG, Karlsruhe

5.4 Antibodies

Table 4. Antibodies

Akt1	Cell Signaling Technology, Inc., Danvers, MA, USA
AlexaFluor® 680 goat anti-mouse IgG, A21058	Invitrogen GmbH, Karlsruhe
AlexaFluor® 750 goat anti-mouse IgG, A21037	Invitrogen GmbH, Karlsruhe
Anti-mouse IgG (H+L) (DyLight® 680 Conjugate), #5470	Cell Signaling Technology, Inc., Danvers, MA, USA
Anti-mouse IgG (H+L) (DyLight® 800 Conjugate), #5257	Cell Signaling Technology, Inc., Danvers, MA, USA
Anti-rabbit IgG (H+L) (DyLight® 680 Conjugate), #5366	Cell Signaling Technology, Inc., Danvers, MA, USA
CDK2 (78B2) Rabbit mAb #2546	Cell Signaling Technology, Inc., Danvers, MA, USA
CDK4 (D9G3E) Rabbit mAb #12790	Cell Signaling Technology, Inc., Danvers, MA, USA
Cyclin D1, sc-246 (HD11)	Santa Cruz Biotechnology, Inc., Dallas, TX, USA
Phospho-FoxO3a (75D8) #2497	Cell Signaling Technology, Inc., Danvers, MA, USA
Phospho-GSK-3β (Ser9) #9336	Cell Signaling Technology, Inc., Danvers, MA, USA
c-myc Antibody (9E10): sc-40	Santa Cruz Biotechnology, Inc., Dallas, TX, USA
Phospho-Tuberin/TSC2 (Ser939) #3615	Cell Signaling Technology, Inc., Danvers, MA, USA

5.5 Molecular biology

All buffers were prepared with bidistilled H_2O.

Table 5. Buffers and solutions for molecular biology

Buffer	Component
IP buffer, pH 7.9	50 mM HEPES 150 mM NaCl 1 mM EDTA 0.5% Nonidet P40 10% Glycerol Phosphatase inhibitor (add prior to use) Protease inhibitor (add prior to use)
Stacking gel buffer	0.5 M Tris, adjusted to pH 6.8 with HCl
Separating gel buffer	1.5 M Tris, adjusted to pH 8.8 with HCl
Running buffer	25 mM Tris 192 mM Glycine 0.1% SDS
Transfer buffer, pH 8.3	25 mM Tris 192 mM Glycine 20% Methanol
5x Protein loading buffer (Laemmli), pH 6.8	10% SDS 50% Glycerol 228 mM Tris hydrochloride 0.75 mM Bromphenol blue 5% 2-Mercaptoethanol
50x Tris acetate EDTA (TAE) buffer, pH 8.5	2 M Tris 50 mM EDTA 5.71% Acetic acid

Table 6. Kits for molecular biology

Kit	**Source**
EndoFree® plasmid maxi kit	Qiagen GmbH, Hilden
QIAamp DNA mini kit	Qiagen GmbH, Hilden
QIAfilter plasmid midi kit	Qiagen GmbH, Hilden
QIAprep® spin miniprep kit	Qiagen GmbH, Hilden
QIAshredder	Qiagen GmbH, Hilden
RNeasy mini kit	Qiagen GmbH, Hilden

Table 7. Bacterial strains

Bacterial strain	**Source**
One Shot® Stbl3™ chemically competent E. coli	Invitrogen GmbH, Karlsruhe

Table 8. Plasmids

pWZL-Neo-Myr-Flag-DEST (#15300)	Addgene, Cambridge, MA, USA
pWZL-Neo-Myr-Flag-AKT1 (#20422)	Addgene, Cambridge, MA, USA
pWZL-Neo-Myr-Flag-AKT3 (#20423)	Addgene, Cambridge, MA, USA
pWZL-Neo-Myr-Flag-ADCK5 (#20416)	Addgene, Cambridge, MA, USA
pWZL-Neo-Myr-Flag-AURKA (#20427)	Addgene, Cambridge, MA, USA
pWZL-Neo-Myr-Flag-CDK2 (#20447)	Addgene, Cambridge, MA, USA

pWZL-Neo-Myr-Flag-CDK4 (#20448)	Addgene, Cambridge, MA, USA
pWZL-Neo-Myr-Flag-CDK5 (#20449)	Addgene, Cambridge, MA, USA
pWZL-Neo-Myr-Flag-CDK7 (#20452)	Addgene, Cambridge, MA, USA
pWZL-Neo-Myr-Flag-CKS1B (#20461)	Addgene, Cambridge, MA, USA
pWZL-Neo-Myr-Flag-EPHA4 (#20483)	Addgene, Cambridge, MA, USA
pWZL-Neo-Myr-Flag-FASTK (#20485)	Addgene, Cambridge, MA, USA
pWZL-Neo-Myr-Flag-ITK (#20507)	Addgene, Cambridge, MA, USA
pWZL-Neo-Myr-Flag-MAP2K5 (#20514)	Addgene, Cambridge, MA, USA
pWZL-Neo-Myr-Flag-PLK1 (#20589)	Addgene, Cambridge, MA, USA
pWZL-Neo-Myr-Flag-PKN1 (#20586)	Addgene, Cambridge, MA, USA
pWZL-Neo-Myr-Flag-PKN2 (#20587)	Addgene, Cambridge, MA, USA
pWZL-Neo-Myr-Flag-PMVK (#20593)	Addgene, Cambridge, MA, USA
pWZL-Neo-Myr-Flag-PRKAA1 (#20595)	Addgene, Cambridge, MA, USA
pWZL-Neo-Myr-Flag-PTK2 (#20610)	Addgene, Cambridge, MA, USA
pWZL-Neo-Myr-Flag-RET (#20614)	Addgene, Cambridge, MA, USA
pWZL-Neo-Myr-Flag-RPS6KA2 (#20621)	Addgene, Cambridge, MA, USA
pWZL-Neo-Myr-Flag-RPS6KA5 (#20622)	Addgene, Cambridge, MA, USA
pWZL-Neo-Myr-Flag-RPS6KA6 (#20623)	Addgene, Cambridge, MA, USA
pWZL-Neo-Myr-Flag-RPS6KB1 (#20624)	Addgene, Cambridge, MA, USA
pWZL-Neo-Myr-Flag-RPS6KB2 (#20625)	Addgene, Cambridge, MA, USA
pWZL-Neo-Myr-Flag-RPS6KL1 (#20626)	Addgene, Cambridge, MA, USA
pWZL-Neo-Myr-Flag-SGK (#20628)	Addgene, Cambridge, MA, USA
pWZL-Neo-Myr-Flag-STK17B (#20635)	Addgene, Cambridge, MA, USA
MSCV-Myc-IRES-RFP (#35395)	Addgene, Cambridge, MA, USA

5.5.1 **Primers**

Oligonucleotides were synthesized by Eurofins MWG GmbH (Ebersberg) and diluted in H_2O to a concentration of 10 µM.

Table 9. Primers used for genotyping

PCR Name	Primer name	Sequence (5' → 3')
Pdk1^{lox}	Pdk1 floxed forward	ATCCCAAGTTACTGAGTTGTGTTGGAAG
	Pdk1 floxed reverse	TGTGGACAAACAGCAATGAACATACACGC

Table 10. Primers for quantitative real time PCR

Gene	Primer name	Sequence (5´→ 3´)	Origin
Cyclophilin	Cyclophilin forward	ATGGTCAACCCCACCGTGT	Mus musculus
	Cyclophilin reverse	TTCTGCTGTCTTTGGAACTTTGTC	
CDK7	CDK7 forward	TTTGCCACCGTTTACAAGGC	Homo sapiens
	CDK7 reverse	AAGGCGGTTCTATTTATACCATCT	
FASTK	FASTK forward	GAAGATGGCGGACTCGGT	Homo sapiens
	FASTK reverse	AGAGAGCAGGACTCGAAGCA	
CKS1B	CKS1B forward	GGACAAATACGACGACGAGGA	Homo sapiens
	CKS1B reverse	AGGGACCAGCTTGGCTATGT	
EPHA4	EPHA4 forward	TCAGGGAGAACTTGGGTGGA	Homo sapiens

	EPHA4 reverse	GCACACTTGGTAGGTTCGGA	
MAP2K5	MAP2K5 forward	ACCAGGGATCTTTAATGCCTCT	Homo sapiens
	MAP2K5 reverse	AACTGGAAGGACGGGCGAAT	
RPS6KA6	RPS6KA6 forward	TCCTGCACAGTTTGAGTTGC	Homo sapiens
	RPS6KA6 reverse	TCATTGCATAGAGCTGCCCA	
STK17B	STK17B forward	CTCGTCCTGTGGCGGC	Homo sapiens
	STK17B reverse	CCCAGGTCTGCTTCTTTAGTCA	
RPS6KL1	RPS6KL1 forward	TGTGACTGGTGGAGCTTTGG	Homo sapiens
	RPS6KL1 reverse	ATTCCTGAAGGGTGGCTCTG	
PKN2	PKN2 forward	GCCAAACTAGCTGGAAACCC	Homo sapiens
	PKN2 reverse	CACACAGAGACCGCCAATCA	
ITK	ITK forward	GAAGTGGAGGTGCTGTTCTCA	Homo sapiens
	ITK reverse	AGTGGTCGCCTGTTGTCTTC	
ADCK5	ADCK5 forward	GAGAAGAGCGGAGCAGTGG	Homo sapiens
	ADCK5 reverse	TCCTGAAGAACACAGCAGGG	
PMVK	PMVK forward	CTTCGTGACCGAGGCGCT	Homo sapiens
	PMVK reverse	TCCTGAGCATACTGTTCCTTGAG	
PLK1	PLK1 forward	TTCGTGTTCGTGGTGTTGGAG	Homo sapiens
	PLK1 reverse	CGGTTTCGGTGCAGGTACT	
RPS6KA2	RPS6KA2 forward	GCCTCTGTTTATTTCCTTTCCTACT	Homo sapiens
	RPS6KA2 reverse	TCCAGGTTGAGATCCTCCTCT	
AURKA	AURKA forward	TGGGTGGTCAGTACATGCTC	Homo sapiens
	AURKA reverse	TCCAAGGCTCCAGAGATCCA	
CDK5	CDK5 forward	TGCAATGGTGACCTCGATCC	Homo sapiens
	CDK5 reverse	GCACATTGCGGCTATGACAG	
RPS6KB1	RPS6KB1 forward	ATTTGCCATGAAGGTGCTTAAA	Homo sapiens
	RPS6KB1 reverse	TCCACGATGAAGGGATGCTT	
AKT3	AKT3 forward	ACCATTGTGAAAGAAGGTTGGG	Homo sapiens
	AKT3 reverse	GGAAGTATCTTGGCCTCCAGT	
PKN1	PKN1 forward	ATGAGAGGCATGAGGTGCAG	Homo sapiens
	PKN1 reverse	CAATGACAGGGTTGCGGAAG	

RPS6KA5	RPS6KA5 forward	TGGCACCAGATATTGTCAGAGG	Homo sapiens
	RPS6KA5 reverse	ACACCCAAACTCCACCAGTC	
SGK	SGK forward	GCACCCTCACTTACTCCAGG	Homo sapiens
	SGK reverse	TCGTTCAGACCCATCCTCCT	
PTK2	PTK2 forward	TGACAGCTACAACGAGGGTG	Homo sapiens
	PTK2 reverse	GTCCAGGTTGGCAGTAGGAG	
RPS6KB2	RPS6KB2 forward	AAGGTGTTCCAGGTGCGAAA	Homo sapiens
	RPS6KB2 reverse	GTGCTGTGTCCTTGGCATTG	
PRKAA1	PRKAA1 forward	GGGTGAAGATCGGCCACTAC	Homo sapiens
	PRKAA1 reverse	TGCCCAGTCAATTCATGTTTGC	
PDPK1	PDPK1 forward	ACGCCCTGAAGACTTCAAGTTTG	Mus musculus
	PDPK1 reverse	GCCAGTTCTCGGGCCAGA	

5.6 Cell culture

Table 11. Cell lines

Cell line	Source
Gryphon™ Eco retroviral packaging cell line	Allele Biotechnology, San Diego, CA, USA

Table 12. Cell culture media and their components

Medium	Components
Cancer cell medium	DMEM 10% FCS (Biochrom AG) 1% Penicillin/Streptomycin
Gryphon™ Eco medium	DMEM 10% FCS (Biochrom AG) 1% Penicillin/Streptomycin 1% L-Glutamine
Freezing medium	70% DMEM 20% FCS 10% DMSO

Table 13. Reagents and kits for cell culture

Reagent/kit	Source
4-hydroxytamoxifen (≥70% Z isomer)	Sigma-Aldrich Chemie GmbH, Munich
Cell proliferation ELISA, BrdU (colorimetric)	Roche Deutschland Holding GmbH, GrenzachWyhlen
Dulbecco's phosphate buffered saline (PBS)	Invitrogen GmbH, Karlsruhe

Fetal calf serum (FCS)	Biochrom AG, Berlin
Fungizone® antimycotic	Invitrogen GmbH, Karlsruhe
G418, Geneticin®	Invitrogen GmbH, Karlsruhe
Giemsa solution	Sigma-Aldrich Chemie GmbH, Munich
MTT reagent	Sigma-Aldrich Chemie GmbH, Munich
Penicillin (10000 units/mL) / Streptomycin (10000 µg/mL) solution	Invitrogen GmbH, Karlsruhe
Puromycin dihydrochloride	Sigma-Aldrich Chemie GmbH, Munich
Effectene® transfection reagent	Qiagen GmbH, Hilden
Trypsin, 0.05% with 0.53 mM EDTA 4Na	Invitrogen GmbH, Karlsruhe

5.7 Software

Table 14

AxioVision 4.8	Carl Zeiss AG, Oberkochen
Excel	Microsoft Corporation, Redmont, WA, USA
GraphPad Prism 5	La Jolla, CA, USA
Nanodrop 2000/2000c Spectrophotometer	Thermo Fisher Scientific, Inc., Waltham, MA, USA
Odyssey® v1.2	Li-Cor Biosciences, Lincoln, NE, USA
StepOne™ v2.3	Applied Biosystems, Inc., Carlsbad, CA, USA

6 Methods

6.1 Cell culture

Murine pancreatic tumour cells were generated from tumour bearing mice and were maintained in cancer cell medium (DMEM supplemented with 10% FCS and 1% penicillin/streptomycin) at 37 °C, 5% CO_2 and 100% humidity.

6.1.1. Passaging of the cells

The medium was aspirated, cells were washed with PBS and detached from the culture dish by incubation with trypsin/EDTA at 37 °C for an appropriate time period. The cell suspension was then transferred into another vessel with medium.

6.1.2. Freezing and thawing of the cells

Trypsinized cells were taken up in fresh medium and centrifuged at 1200 rpm for 5 minutes (min).

The pellet was dissolved in ice-cold freezing medium (70% DMEM, 20% FCS, 10% DMSO), transferred to CryoPure tubes, frozen at -80°C and after a few days processed to liquid nitrogen, where the cells were stored until further use.

Cells were thawed at room temperature (RT) and put in a vessel with medium. On the next day, medium was changed in order to remove DMSO.

6.1.3. Treatment of the cells with EtOH and 4-OHT

Cells were treated with Ethanol (EtOH) (control cells) or 600 nM 4-hydroxytamoxifen (4-OHT) for 8 days in order to delete *loxP*-flanked sequences through the activation of $CreER^{T2}$. Cells were then seeded for a variety of assays.

6.1.4. Cell viability

In order to measure cell viability, MTT and clonogenic assay were performed on cells treated for 8 days with EtOh and 4-OHT with a concentration of 600 nM in a 10 cm dish.

6.1.4.1. MTT assay

Cells were seeded in a 96-well plate with three different concentrations (between $5x10^2$ and $2x10^3$ cells) as triplicate per condition. On the next day, 10 µL of MTT reagent (3-(4,5-dimethylthiazol-2-yl)-2,5-diphenyl tetrazolium bromide) were added to the cells. MTT is a pale yellow substrate that is cleaved by living cells to yield a dark blue formazan product. Cells were then incubated for 4 h at 37 °C and at the end of this time, the MTT formazan produced in wells containing live cells will appear as black, fuzzy crystals on the bottom of the well. Just before reading, the wells were filled with 200 µL EtOH/DMSO solution. The absorbance was measured on an ELISA plate reader with a wavelength of 570 nm (and a reference wavelength of 630 nm). Absorbance is directly proportional to the number of cells. As a result, MTT assay is a test to measure cell viability indirectly.

6.1.4.2. Clonogenic assay

Clonogenic assay or colony formation assay is an *in vitro* cell survival assay based on the ability of a single cell to form a colony.

Cells were seeded in 6-well plates in a concentration of $1x10^3$ cells in cancer cell medium. After 2-3 weeks the colonies were fixed with cold methanol stained wih Giemsa (diluted 1:20-1:40).

6.1.5. ^{F18}-FDG uptake assay

For quantification of uptake of ^{F18}-FDG into tumour cells, $1x10^5$ cells were seeded into 24-well plates as quadruples for each condition. On the following day, the cell culture medium was removed, cells were washed twice with glucose-free medium and were incubated in glucose-free cell culture medium that was supplemented with ^{F18}-FDG at a radioactivity of 0.185 MBq/mL. After 60, 90 and 120 min plates were put on ice, washed twice with ice cold PBS and cells were detached with 1 M NaOH and harvested for glucose uptake measurements using a gamma counter. Tumour cell uptake was referred to the ^{F18}-FDG standard and cell uptake was displayed as percent of the standard (uptake in %). ^{F18}-FDG uptake assays were performed in cooperation with Benedikt Feuerecker.

6.1.6. Plasmid Isolation

Plasmid Isolation was done according to QIAGEN Kit protocol.

6.1.7. Retrovirus production: Transfection of EcoGryphon cells

For the transfection EcoGryphon cells (Allelebiotech) were used. The line was created by placing conctructs capable of producing retroviral proteins into 293T cells (a human embryonic kidney line transformed with adenovirus E1a and carrying a temperature sensitive T antigen co-selected with neomycin). On the day before transfection, EcoGryphon cells were seeded in 10cm dishes (between $1x10^5$ and $5x10^6$). For the transfection, 3 µg of plasmid DNA was filled up with EC buffer to 300 µL and condensed by addition of 48 µL of enhancer. The mix was vortexed and incubated for 2-5 min. Then, 30 µL Effectene were added and, after being vortexed for 10 seconds, the solution was incubated for 5-10 min. The formed Effectene®-DNA complexes were then mixed with medium and added dropwise to the cells. After 48h the viral supernatant was used for the transduction.

6.1.10 Transduction

On the day before transduction, target cells were seeded in a 12-well plate in a concentration between 1-$2x10^5$ cells. For retroviral transduction, the viral supernatant was centrifugated at RT for 5 min by 1250 rpm, filtered with a 0.45 µm filter to remove any packaging cells that were collected during harvesting and mixed with Polybrene at a concentration of 8 µg/mL in order to enhance the efficiency of the transfection. 1 mL of the supernatant was then given to the target cells. The same procedure was repeated on the day after. After two days, selection was carried out with neomycin.

6.2. Molecular biology

6.2.1. Polymerase chain reaction (PCR)

A PCR pre-mix containing buffer (see Table 15), polymerase and dNTPs was used. The standard PCR reaction conditions are shown in the table 16. PCR products were stored at 4 °C until further analysis by gel electrophoresis.

Table 6.15. Composition of pre-mix for PCR

Solution	Volume for one reaction
Distilled water	4.375 µL
10 X buffer S	2.5 µL
30% sucrose	2.5 µL
SucRot	2.5 µL
PeqTaq	0.125 µL
dNTPs (10 µM each)	0.5 µL

Table 6.16. Reaction mix and conditions for standard PCR.

Reaction mix		Conditions		
12.5 µL	PCR pre-mix	95°C	3 min	
0.5-2 µL	forward primer (10 µM)	95°C	45 s	40 x
0.5-2 µL	reverse primer (10 µM)	55-72°C	60 s	
1.5 µL	DNA	72 °C	90 s	
Ad 25 µL	distilled water	25 °C	hold	

6.2.2.RNA isolation and cDNA synthesis

RNA isolation from cells. Cells were treated for 8 days with EtOH or 4-OHT at the concentration of 600 nM in a 10 cm dish. Medium was aspirated and 600 µL of RLT buffer containing 6 µL 2-mercaptoethanol were added to the plate, the lysate was collected with a scraper and kept at -80°C until use. For RNA isolation, QIAshredder columns and the RNeasy mini kit were employed. DNA was digested using the RNase-free DNase set. RNA concentration was measured with the spectrophotometer NanoDrop 1000. Samples were stored at -80°C.

cDNA synthesis was carried out with the TaqMan® reverse transcription reagents. 1 µg of mRNA was used for generation of 30 µL cDNA, which was stored at -20°C.

6.2.3. Quantitative real time PCR

Primer design. The DNA sequences were acquired at www.ncbi.nlm.nih.gov/nucleotide. Primers for quantitative real time PCR (qPCR) were

generated using Primer-blast at the NCBI homepage (www.ncbi.nlm.nih.gov/tools/primer-blast).

The length of the amplicons was 50–150 bp and the binding sites of forward and reverse primer were always separated by an intron to avoid unwanted amplification of genomic DNA.

Quantitative real time PCR was performed with the StepOnePlus™ real time PCR system. As fluorescent DNA binding dye, QuantiFast® SYBR® green PCR master mix was used in a 25 µL mixture. 300 nM both forward and reverse primer were added. mRNA expression was analysed on 5 µL cDNA in triplicate. All mRNA expression values were normalized to the housekeeping gene Cyclophillin (CypA). Afterwards, a melt curve was performed to exclude unwanted primer dimerization. Data analysis was done with StepOne™ software (Applied Biosystems, Inc., Carlsbad, CA, USA) and Excel (Microsoft Corporation, Redmont, WA, USA). Either a standard curve was included as well, or further analysis was performed according to the $2^{-\Delta\Delta Ct}$ method (see below).

$2^{-\Delta\Delta Ct}$ analysis method. If primer efficiency was between 1.8 and 2.2, the $2^{-\Delta\Delta Ct}$ method (Pfaffl, 2001) was applied for relative mRNA expression analysis, otherwise, a standard curve was used. ΔCt was calculated as follows:

$$C_t\,[\text{gene of interest}] - C_t\,[\text{control}] = \Delta C_t$$
$$\Delta C_t[\text{treated sample}] - \Delta C_t[\text{reference sample}] = \Delta\Delta C_t$$

$2^{-\Delta\Delta Ct}$ was used for further data analysis.

Standard curve.

In order to assess the human kinase expression in transduced cells compared to untransduced cells, standard curve were performed. Serial dilutions in TE buffer were prepared from the isolated plasmid DNA according to Table 6.17. 5 µL of 5 standards for each gene of interest were included into every run.

Table 6.17: Standard curve dilution for quantitative real time PCR.

Name	Molecules per µL	Molecules per 5 µL
S 0	150000	750000
S I	30000	120000
S II	6000	30000

Name	Molecules per µL	Molecules per 5 µL
S III	1200	6000
S IV	240	1200

6.2.4. Protein isolation

Once the treatment was over, medium was aspired and the dish was washed twice with cold PBS. Afterwards, 150 µL IP buffer containing protease inhibitor and phosphatase inhibitor was added. Proteins were harvested on ice with a cell scraper and put in liquid nitrogen. Then the lysates were stored at -80 °C. Shortly before use, they were centrifuged for 20 min at 14000 rpm at 4 °C.

Western Blot

Protein concentration was assessed by Bradford assay. Bradford reagent was diluted 1:5 with water and 300 µL were put in each well. Every sample was analysed in triplicate and 1 µL of each was added. As a reference, serial dilutions of BSA were used. The concentration was measured by the reader Winread/Anthos1 at 600 nm.
Afterwards, the proteins were set at the same concetration by adding IP buffer and Lämmli. Proteins were denaturated at 95 °C for 5 min and then stored at -20°C.

SDS-Page

Separating gel was prepared at a concentration between 10 and 12%. All the reagent were mixed apart from TEMED and 10% APS, which were put at last. The concentration are the same used in the Table 6.18. After pouring into a gel caster, Isopropanol was added in order to allow the gel to polymerize. When separating gel was polymerized, TEMED and 10% APS were added to the stacking gel, mixture isopropanol was taken out and stacking gel was poured.
120-150 µg of the proteins were loaded in the single wells. Electricity was applied at 100 V and, once the proteins overcame the stacking gel, it was increased to 120 V. The protein separation was carried out for 2-4 h according to the molecular weight of the protein to analyse.

Table 6.18 Recipe for the SDS polyacrylamide gels

Compound	10% separating gel	12% separating gel	Stacking gel
H_20	6150 µL	5100 µL	4500 µL
Separating gel buffer	3900 µL	3900 µL	-
Stacking gel buffer	-	-	1950 µL
Rotiphorese® gel 30	4950 µL	6000 µL	1125 µL
10% SDS	150 µL	150 µL	75 µL
10% APS	75 µL	75 µL	37.5 µL
TEMED	22.5 µL	22.5 µL	15 µL

6.2.1. Blotting

The gel was blotted onto a PDVF membrane, which was previously activated with methanol. Blotting was performed either for 2 h at 350 mA or for 16 h at 90 mA. After blotting, the membrane was incubated with a 5% BSA/PBS blocking solution for 1 h, in order to prevent unwanted binding of the antibody. Afterwards, the first antibody was applied overnight at 4°C while being slowly rocked. The antibody was generally diluted 1:1000 with the blocking solution. It was washed three times with a PBS/0.1%Tween solution and afterwards, the second antibody, generally 1:5000 diluted, was applied for 1 h and slowly rocked in the dark. Subsequently, the membrane was washed three times every fifteen min and detected either at 700 nm or 800 nm wavelength with the Odyssey infrared imaging system. As a loading control, β-actin or α-tubulin were generally used.

6.3. Statistical analysis

Graphical depiction, data correlation and statystical analysis were performed with GraphPad Prism 5. If not specified otherweise, data were obtained from at least three indipendent experiments and are presented as arithmetic mean ± standard deviation (SD) or standard error of the mean (SEM). Cell culture-based assays were performed

in triplicate. To calculate statistical differences between certain data sets, two-tailed Student's t test was employed.

To calculate statistical differences between certain data sets, normality and variance were analyzed and a two-tailed Student's t test was employed. Statistical comparisons between MTT curves were obtained with a two-way analysis of variance (ANOVA) test.

7. Results

7.1. An inducible Pdk1-KO system *in vitro*

The used mouse model *Pdx1-Flp;FSF-Kras*$^{G12D/+}$*;FSF-R26*$^{CAG\text{-}CreERT2/+}$*;Pdk1*$^{lox/lox}$ is here abbreviated *Pdk1*$^{lox/lox}$ or referred to as *Pdk1*-KO.

In order to delete *Pdk1*, PDAC cell lines from *Pdk1*$^{lox/lox}$ mice were treated for 8 days with 4-OHT to activate the CreER^{T2} expression. As shown in Figure 7-1B (b,d), *Pdk1* is completely recombined after 8 days treatment with 4-OHT.

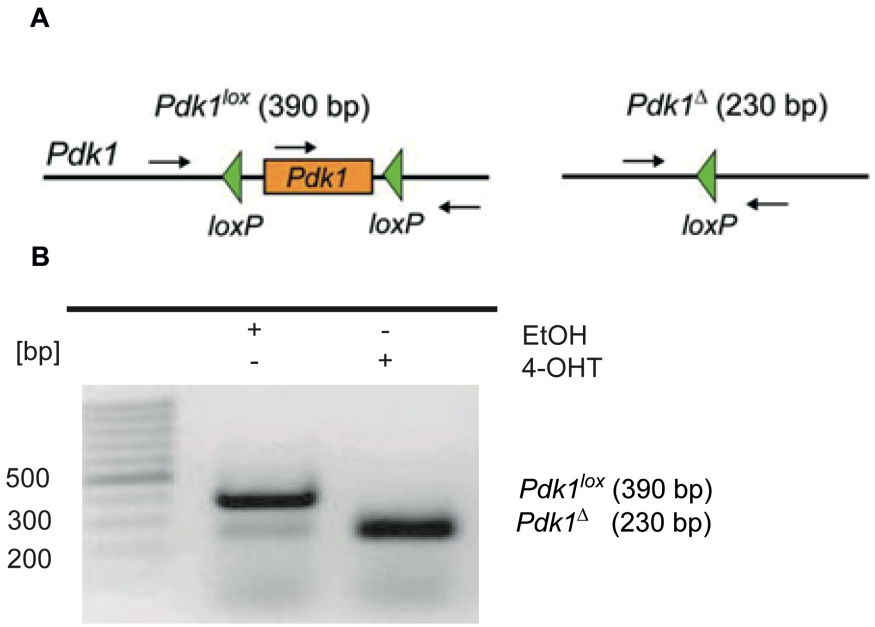

Figure 7-1. **PCR analysis of *Pdk1*$^{lox/lox}$ DNA.** (A) genotyping strategy to detect *Pdk1* alleles. (B) PCR analysis of recombined (*Pdk1*$^{\Delta}$) and not-recombined (*Pdk1*^{lox}) *Pdk1*$^{lox/lox}$ DNA from a *Pdk1*$^{lox/lox}$;*LSL-Trp53*$^{R172H/+}$ mouse cell line treated for 8 days with either EtOH (control cells) or 600 nM 4-OHT (n=1).

7.2. Akt1-myr expression can rescue Pdk1-KO phenotype

Since AKT represents one of the main targets of Pdk1, which mediates the phosphorylation on the T308 residue, the effect of the expression of its myristoylated form (Akt1-myr and Akt3-myr) was analysed. Akt1-myr was the only analysed myristoylated kinase which was able to completely rescue Pdk1 loss.

This result was validated on further two cell lines, which were differing from the former only for the *Trp53* allele (*Trp53*$^{frt/+}$ instead of *Trp53*$^{R172H/+}$). The cells expressing Akt1-myr treated with 4-OHT were forming as many colonies and were growing as

fast as cells treated with EtOH (Figure 7-2A, B). The Akt1-myr expression was proven by the Western Blot (Figure 7-2D).

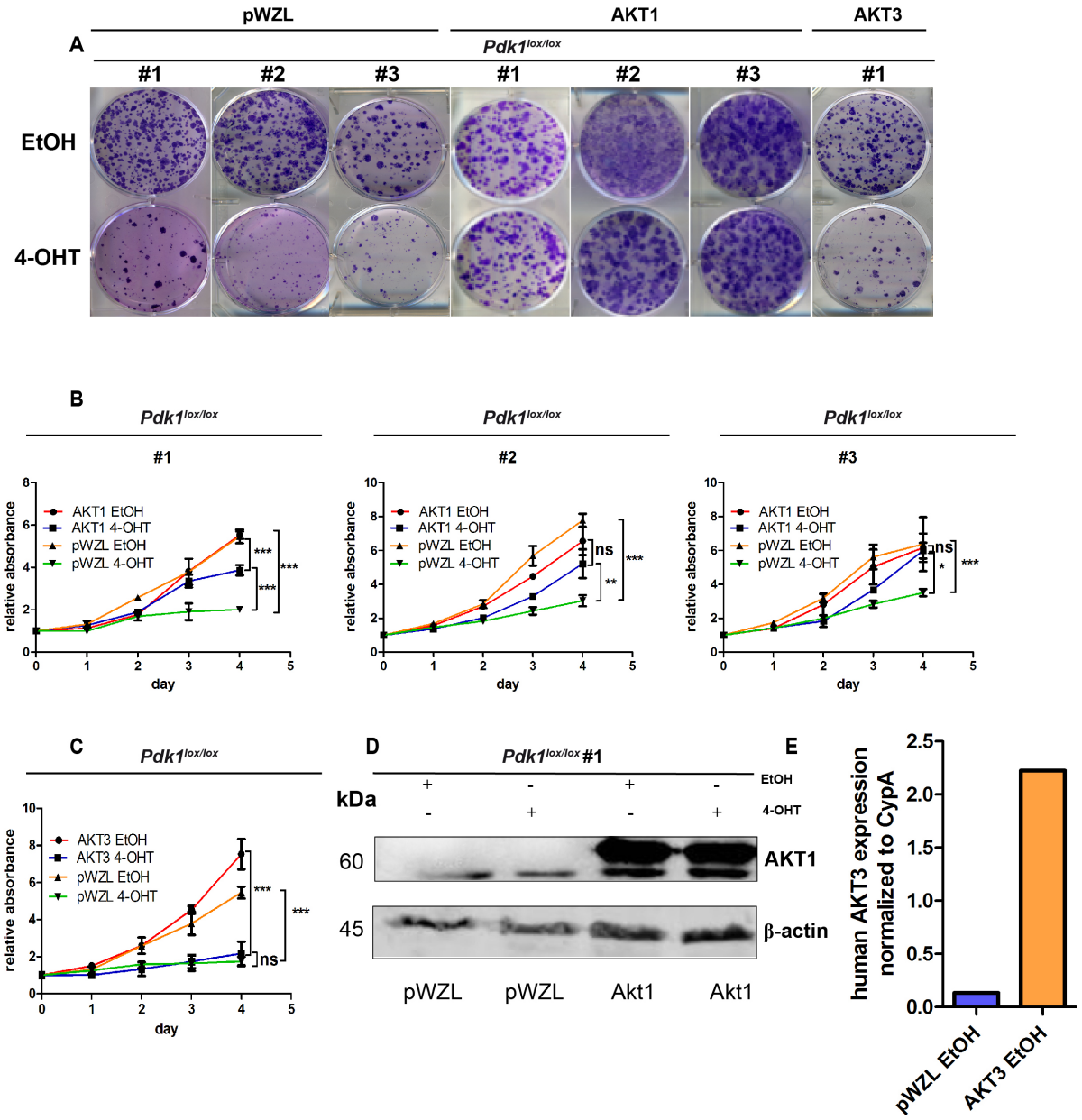

Figure 7-2. Expression of Akt1-myr and Akt3-myr on *Pdk1*$^{lox/lox}$ cell lines. (A) Clonogenic assay of *Pdk1*$^{lox/lox}$*;LSL-Trp53*$^{R172H/+}$ cells (#1) and *Pdk1*$^{lox/lox}$*;Trp53*$^{frt/+}$ cells (#2, #3) expressing AKT1-myr and AKT3-myr treated with EtOH and 4-OHT in comparison to empty vector (pWZL) A representative picture is shown, n = 3 replicates. (B) MTT assays of *Pdk1*$^{lox/lox}$*;LSL-Trp53*$^{R172H/+}$ cell line (#1) and *Pdk1*$^{lox/lox}$*;Trp53*$^{frt/+}$ cells (#2, #3) expressing AKT1-myr treated with EtOH and 4-OHT treated ones in comparison to empty vector (pWZL). Data are shown as mean ± SD; n = 3 replicates. ***p < 0.001, **p < 0.01, *p < 0.05, ns p > 0.05, stepwise two-way ANOVA with Bonferroni correction (n=3). (C) MTT assays of *Pdk1*$^{lox/lox}$*;LSL-Trp53*$^{R172H/+}$ cell line expressing AKT3-myr treated with EtOH and 4-OHT treated ones in comparison to empty vector (pWZL) (n=3). (D) Western Blot analysis showing the expression of AKT1-myr in *Pdk1*$^{lox/lox}$*;LSL-Trp53*$^{R172H/+}$ cell line treated with EtOH and 4-OHT in comparison to empty vector (pWZL); ß-actin served as loading control. (E) qPCR showing the expression of AKT3-myr in *Pdk1*$^{lox/lox}$*;LSL-Trp53*$^{R172H/+}$ cell line.

The expression of Akt3-myr, on the other hand, was not able to rescue Pdk1 loss and its expression was functional, as verified by the qPCR (Figure 2-E).
To summarise, these results show that Akt1 can rescue completely the Pdk1-KO phenotype.

7.2.1. GSK3β represents a major downstream effector of Akt1

Since Akt1 has several targets, we investigated which ones were hyperphosphorylated when Akt1-myr was expressed (Figure 7-3 B, C). Among the analysed downstream kinases, an hyperphosphorylation of Gsk3β was observed in all the three *Pdk1*$^{lox/lox}$ cell lines. Moreover, there was no difference between cells treated with EtOH and 4-OHT leading to the conclusion that the Akt1-myr expression is not only able to rescue the
Pdk1-loss phenotype, but also that Gsk3β plays a key role as a downstream effector.
The other downstream effectors that were analysed are cyclin D1, p70S6K, pTSC-2 and
P-FoxO3a, but in these cases no difference in the phosphorylation or protein expression between cells expressing Akt1-myr and pWZL was observed (Figure 7-3B).

7.2.2. Effects of Akt1-myr expression on glucose metabolism

In addition to reduced cell viability, previous experiments (C. Veltkamp) have shown an impairment in glucose metabolism of *Pdk1*-KO cell lines.
Since a higher cell proliferation rate leads to an increased consumption of glucose as an energy source, we performed glucose metabolism assays on Akt1-myr expressing cell lines compared with control cell lines (Figure 7-3 A).
The cells were treated for 8 d with EtOH or 4-OHT and a glucose uptake assay was performed using radioactively labelled glucose (^{F18}-FDG) for 60, 90 and 120 min.
Upon *Pdk1* ablation, both cells lines showed a reduction in glucose uptake. However, cells expressing Akt1-myr showed a much stronger glucose metabolism in comparison to control cells, leading to the conclusion that Akt1 can stimulate glucose metabolism in the absence of Pdk1.

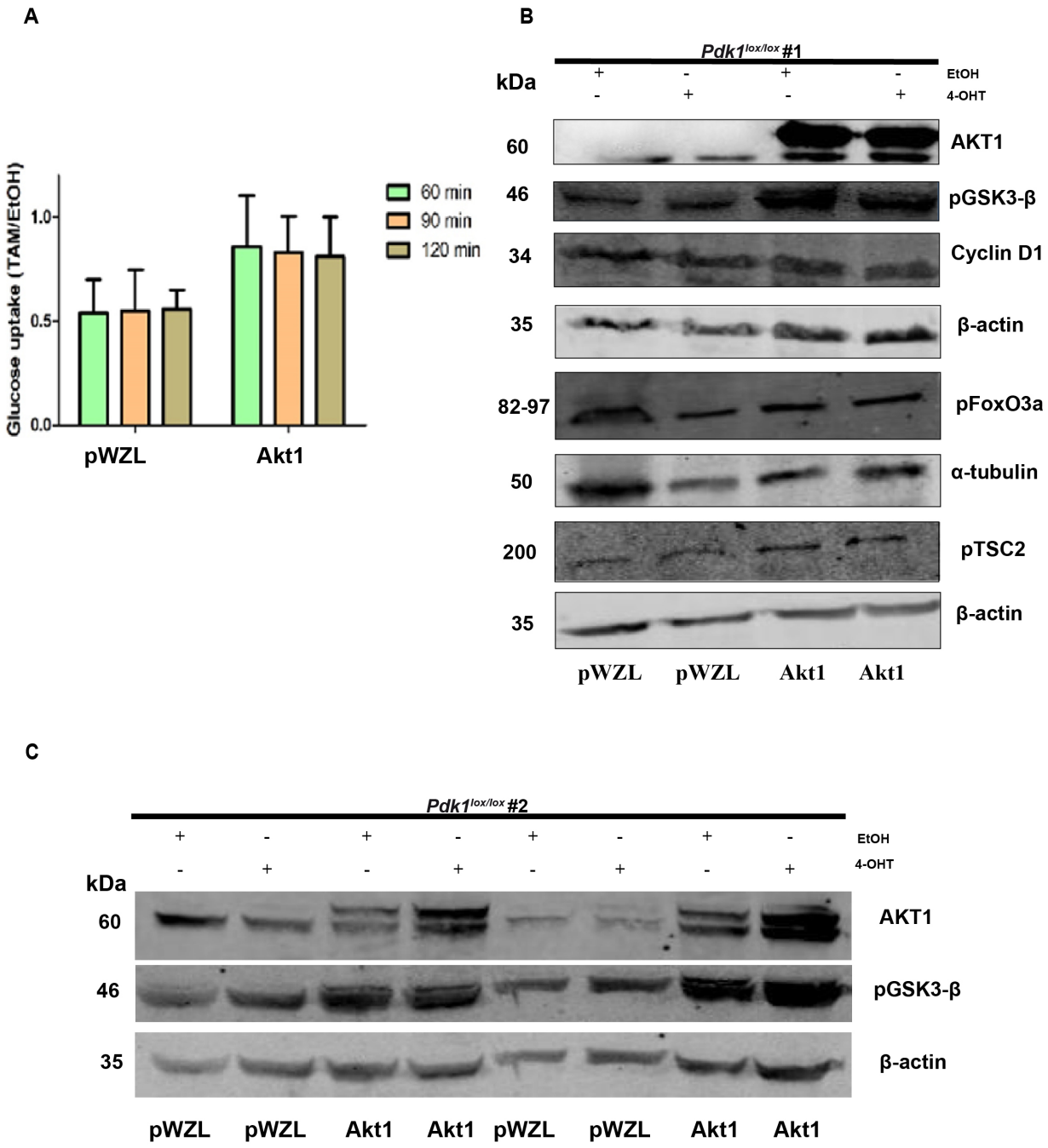

Figure 7-3 Downstream pathways of Akt1 (A) Effects on glucose metabolism in cells expressing Akt1-myr (Akt1) in comparison to empty vector (pWZL) (n=1). (B) Immunoblot analysis of PI3K/AKT downstream signaling in EtOH- and 4-OHT-treated *Pdk1*$^{lox/lox}$;*LSL-Trp53*$^{R172H/+}$ cell lines expressing Akt1-myr (Akt1) compared to empty vector (pWZL). α-tubulin and ß-actin served as loading control. Western blot of proteins of the pathway in cells comparison to control cells (pWZL) respectively treated with EtOH (control cells) and 4-OHT (n=1). (C) Western blot showing the expression of Akt1 and pGSK3β in *Pdk1*$^{lox/lox}$;*Trp53*$^{frt/+}$ cells expressing Akt1-myr (Akt1) in comparison to empty vector (pWZL) treated with EtOH and 4-OHT respectively (n=1). ß-actin served as loading control.

7.3. RPS6KA5-myr expression can partially rescue Pdk1-KO phenotype

7.3.1. RPS6KA5

The ribosomal protein S6 kinase family is involved in several kinds of tumours.
RPS6Kα proteins activate mitosis, whereas RPS6Kβ proteins are involved in cell growth and regulation and insulin regulation as well (Slattery et al., 2011). Moreover, they both require Pdk1 phosphorylation for their activation (Jensen et al., 1999).
In this study, kinases belonging to both RPS6Kα (RPS6KA2 (RSK3), RPS6KA5, RPS6KA6 (RSK4)) and RPS6Kβ (RPS6KB1 (p70s6k), RPS6KB2) families as well as RPS6KL1, were analised. Among these, only RPS6KA5 (Ribosomal Protein S6 Kinase, A5), which is required for the mitogen or stress-induced phosphorylation and regulation of multiple transcription factors, showed a partial rescue of the Pdk1-KO phenotype.
RPS6KA5-myr cells treated with 4-OHT formed almost as much colonies as cells treated with EtOH (Figure 7-4A). However, RPS6KA5-myr cells treated with 4-OHT did not grow as fast as RPS6KA5-myr cells treated with EtOH (Figure 7-4 B,C). The result was validated on a further cell line.
To summarize, this experiment demonstrates that RPS6KA5 is able to rescue the *Pdk1*-KO phenotype partially, suggesting that RPS6KA5 is an important Pdk1 effector molecule in PDAC. The expression of RPS6KA5-myr was verified by qRT -PCR (Figure 7-4D,E).

7.4. CKS1B can almost completely rescue Pdk1-KO phenotype

CKS1B (Cdc28 protein kinase regulatory subunit 1B) plays an important role in cell cycle regulation. It enhances the interactions between SKP2 and p27KIP1 (CDK inhibitor), leading to its proteasomal-mediated degradation and consequent cell cycle progression (Shi et al., 2010). CKS1B is not known to be associated with PI3K pathway. Furthermore, its involvement in pancreatic cancer is not studied yet.
CKS1B-myr was expressed in *Pdk1*$^{lox/lox}$ cells and it showed to rescue almost completely the Pdk1-KO phenotype, as shown in the MTT and clonogenic assay (Figure 7-5 A,B,C,D,E). This result was validated in two additional cell lines. The expression was demonstrated on the mRNA level (Figure 7-5 F,G,H).

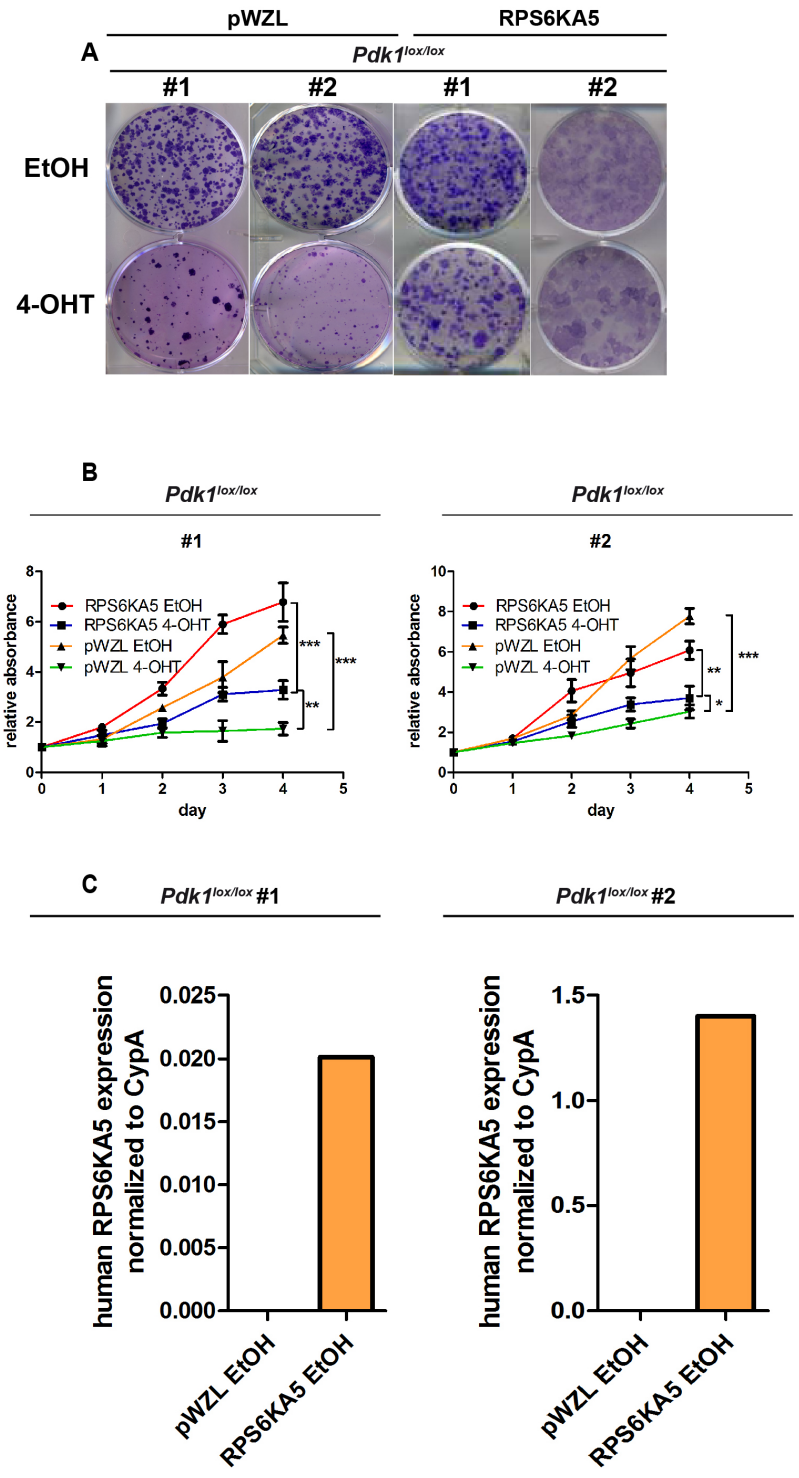

Figure 7-4: Expression of RPS6KA5-myr on *Pdk1*$^{lox/lox}$ cell lines (A) Clonogenic assay of *Pdk1*$^{lox/lox}$*;LSL-Trp53*$^{R172H/+}$ cells and *Pdk1*$^{lox/lox}$*;Trp53*$^{frt/+}$ cells expressing RPS6KA5-myr treated with EtOH and 4-OHT in comparison to empty vector (pWZL). A representative picture is shown, n = 3 replicates. (B) MTT assays of *Pdk1*$^{lox/lox}$*;LSL-Trp53*$^{R172H/+}$ cell line (#1) and *Pdk1*$^{lox/lox}$*;Trp53*$^{frt/+}$ cells (#2) expressing RPS6KA5-myr treated with EtOH and 4-OHT in comparison to empty vector (pWZL). Data are shown as mean ± SD; n = 3 replicates. ***p < 0.001, **p < 0.01, *p < 0.05, ns p > 0.05, stepwise two-way ANOVA with Bonferroni correction (n=3) .
(C) qPCR showing the expression of RPS6KA5-myr in *Pdk1*$^{lox/lox}$*;LSL-Trp53*$^{R172H/+}$ cell line (#1) and in *Pdk1*$^{lox/lox}$*;Trp53*$^{frt/+}$ cells (#2).

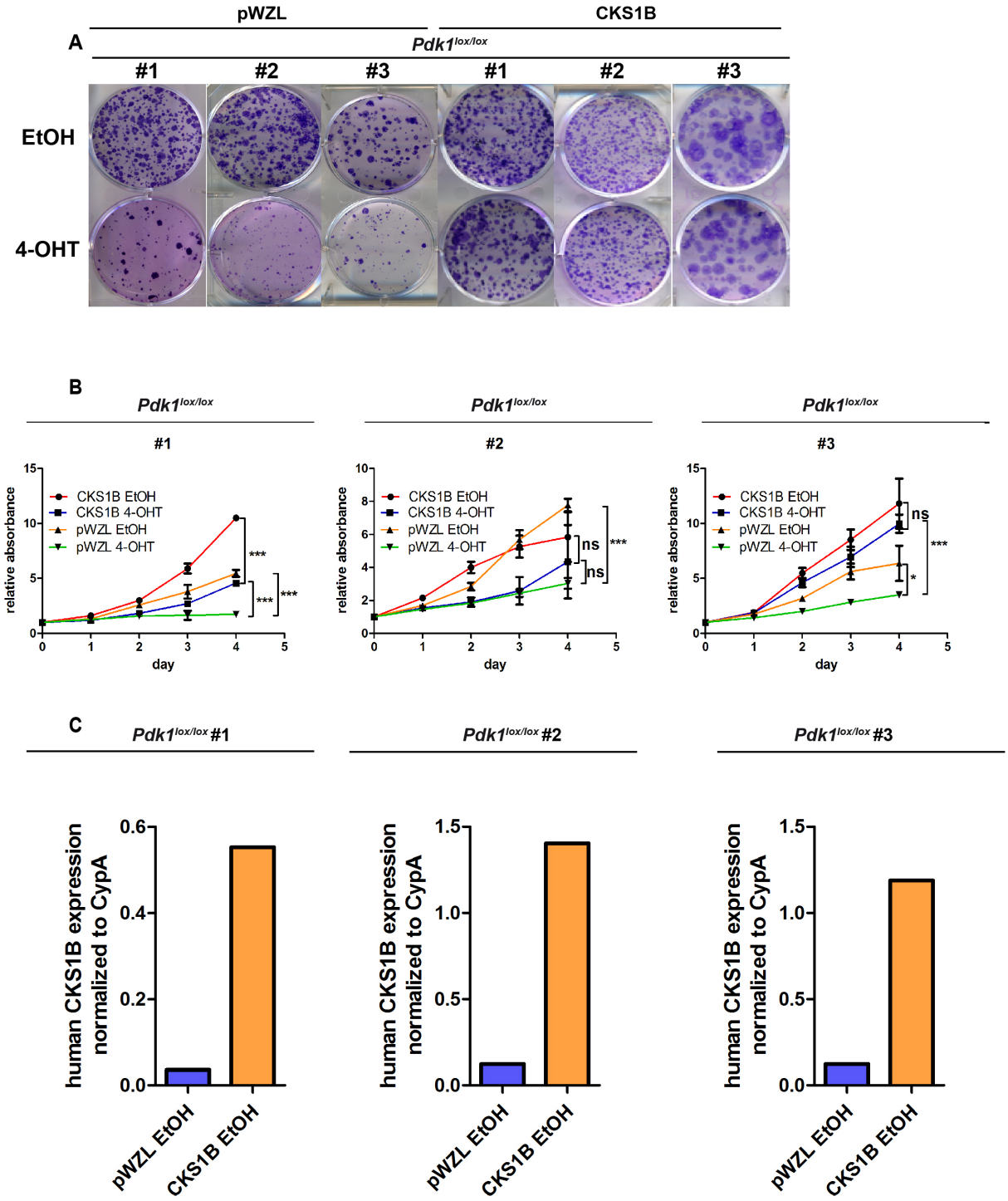

Figure 7-5. Expression of CKS1B-myr on *Pdk1*$^{lox/lox}$ cell lines (A) Clonogenic assay of *Pdk1*$^{lox/lox}$*;LSL-Trp53*$^{R172H/+}$ cells (#1) and *Pdk1*$^{lox/lox}$*;Trp53*$^{frt/+}$ cells (#2, #3) expressing CKS1B-myr treated with EtOH and 4-OHT in comparison to empty vector (pWZL). A representative picture is shown, n = 3 replicates. (B) MTT assays of *Pdk1*$^{lox/lox}$*;LSL-Trp53*$^{R172H/+}$ cell line (#1) and *Pdk1*$^{lox/lox}$*;Trp53*$^{frt/+}$ cells (#2, #3) expressing CKS1B-myr treated with EtOH and 4-OHT in comparison to empty vector (pWZL). Data are shown as mean ± SD; n = 3 replicates. ***p < 0.001, **p < 0.01, *p < 0.05, ns p > 0.05, stepwise two-way ANOVA with Bonferroni correction (n=3). (C) qPCR showing the expression of CKS1B-myr in *Pdk1*$^{lox/lox}$*;LSL-Trp53*$^{R172H/+}$ cell line (#1) and *Pdk1*$^{lox/lox}$*;Trp53*$^{frt/+}$ cells (#2, #3).

7.5. Effect of expression of other myristoylated kinases on *Pdk1*$^{lox/lox}$ cell lines

In this study the effects of the expression of the following myristoylated kinases on *Pdk1*$^{lox/lox}$ cell lines were analysed: ADCK5, AURKA, CDK4, CDK5, CDK7, EPHA4, FASTK, ITK, MAP2K5, PKN1, PKN2, PLK-1, PMVK, PRKAA1, PTK2, RET, RPS6KA6, RPS6KB1, RPS6KB2, RPS6KL1, SGK, STK17B (Figure 7-6, 7-7, 7-8, 7-9, 7-10, 7-11). As shown in the clonogenic assay and MTT assay, the following kinases were not able to rescue the Pdk1-KO phenotype.

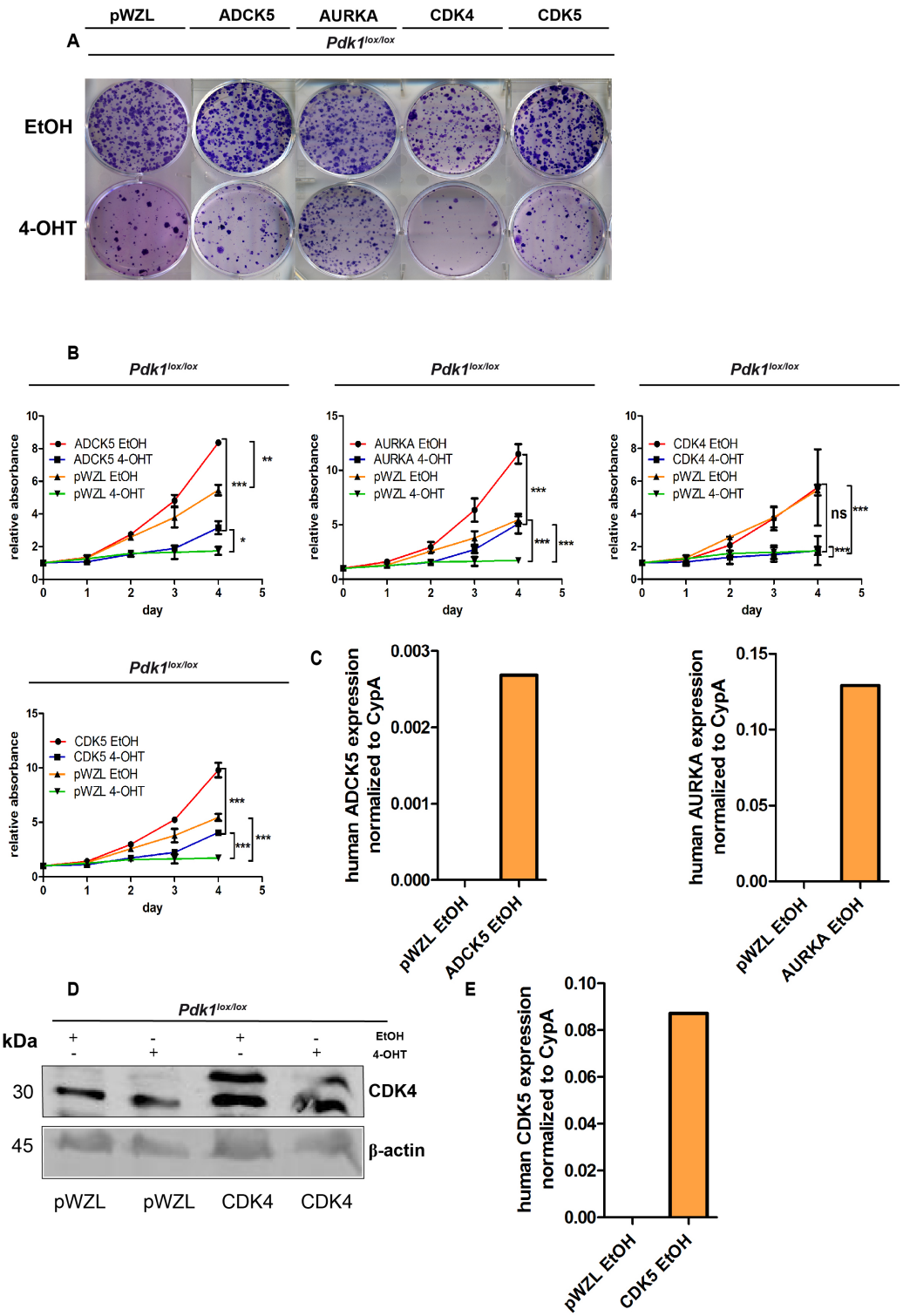

Figure 7-6 Expression of ADCK5-myr, AURKA-myr, CDK4-myr and CDK5-myr on *Pdk1*$^{lox/lox}$ cell line (A) Clonogenic assay of *Pdk1*$^{lox/lox}$*;LSL-Trp53*$^{R172H/+}$ cells expressing ADCK5-myr, AURKA-myr, CDK4-myr and CDK5-myr treated with EtOH and 4-OHT. A representative picture is shown, n = 3 replicates. (B) MTT assay of *Pdk1*$^{lox/lox}$*;LSL-Trp53*$^{R172H/+}$ cells expressing ADCK5-myr, AURKA-myr, CDK4-myr and CDK5-myr treated with EtOH and 4-OHT in comparison to empty vector (pWZL). Data are shown as mean ± SD; n = 3 replicates. ***p < 0.001, **p < 0.01, *p < 0.05, ns p > 0.05, stepwise two-way ANOVA with Bonferroni correction (n=3).

(n=3). (C,E) qPCR showing the expression of ADCK5-myr (C), AURKA-myr (C) and CDK5-myr (E) in *Pdk1*$^{lox/lox}$*;LSL-Trp53*$^{R172H/+}$ cell line. (D) Western blot showing the expression of CDK4 in *Pdk1*$^{lox/lox}$*;LSL-*

Trp53$^{R172H/+}$ cells treated with EtOH and 4-OHT in comparison to empty vector (pWZL). ß-actin served as loading control.

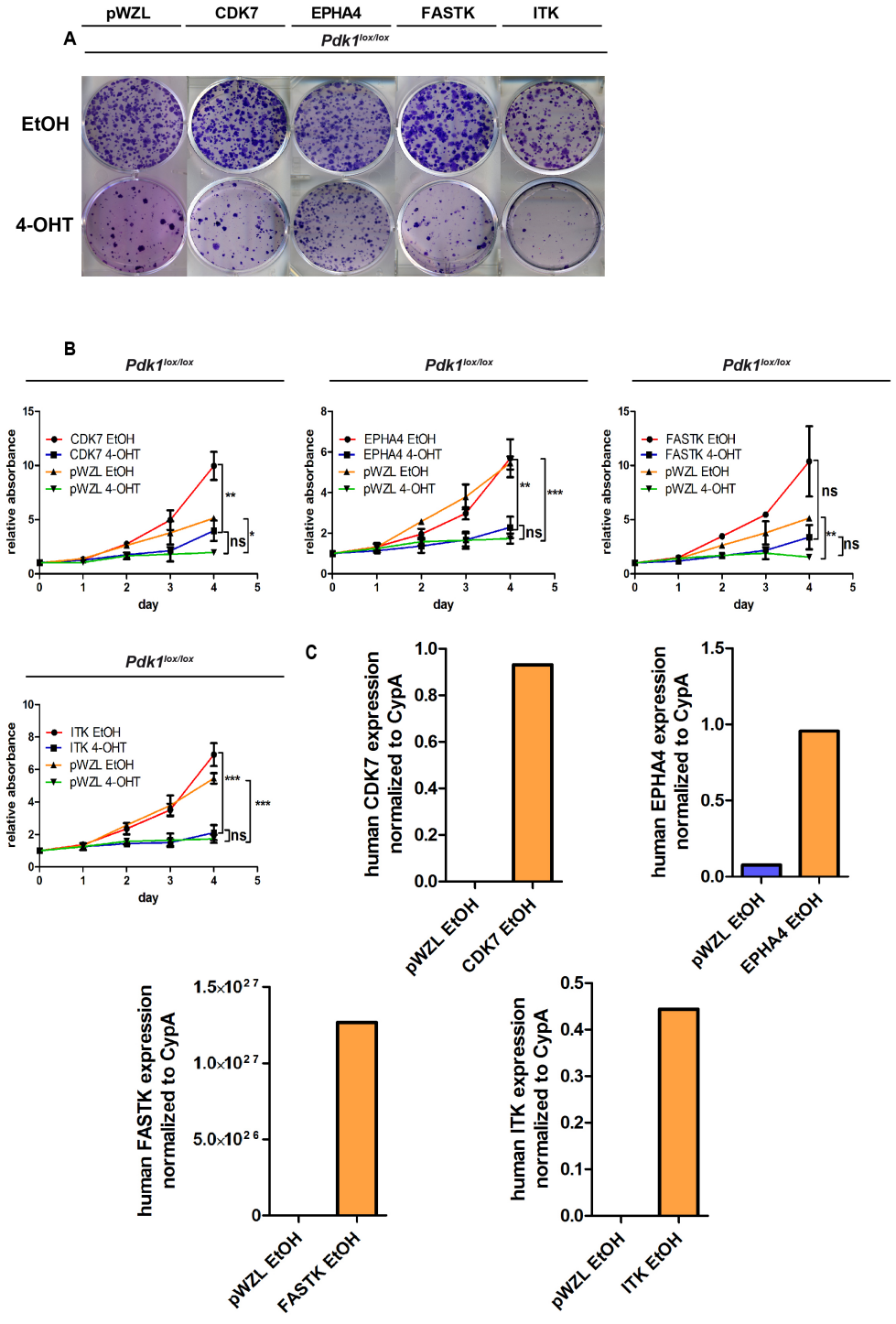

Figure 7-7: Expression of CDK7-myr, EPHA4-myr, FASTK-myr and ITK-myr on *Pdk1*$^{lox/lox}$ cell line
(A) Clonogenic assay of *Pdk1*$^{lox/lox}$*;LSL-Trp53*$^{R172H/+}$ cells expressing CDK7-myr, EPHA4-myr, FASTK-myr and ITK-myr treated with EtOH and 4-OHT in comparison to empty vector (pWZL). A representative picture is shown, n = 3 replicates. (B) MTT assay of *Pdk1*$^{lox/lox}$*;LSL-Trp53*$^{R172H/+}$ cells expressing CDK7-myr, EPHA4-myr, FASTK-myr and ITK-myr treated with EtOH and 4-OHT in comparison to empty vector (pWZL). Data are shown as mean ± SD; n = 3 replicates. ***p < 0.001, **p < 0.01, *p < 0.05, ns p > 0.05,

stepwise two-way ANOVA with Bonferroni correction (n=3). (C) qPCR showing the expression of CDK7-myr, EPHA4-myr, FASTK-myr and ITK-myr in *Pdk1*$^{lox/lox}$;*LSL-Trp53*$^{R172H/+}$ cell line.

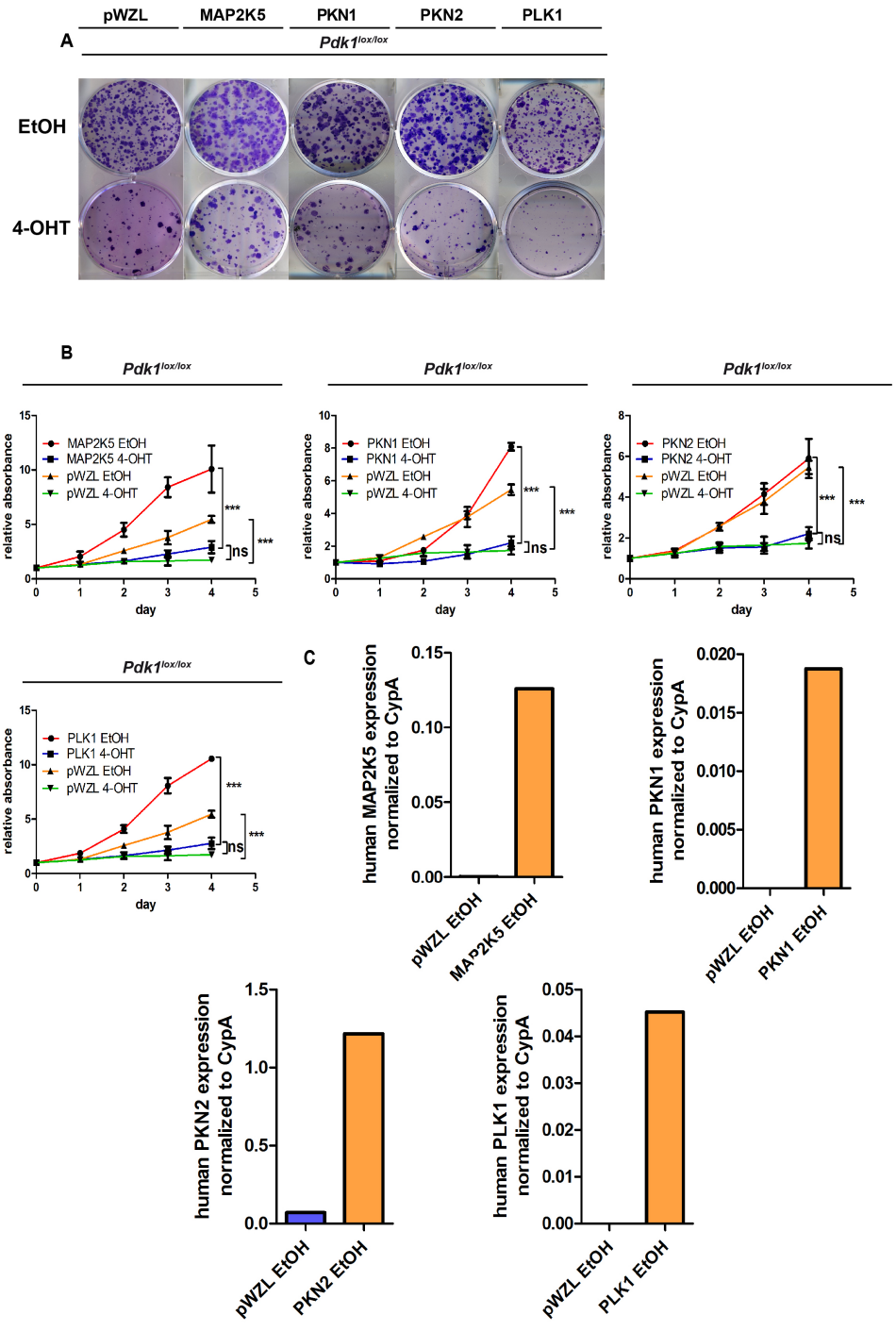

Figure 7-8: Expression of MAP2K5-myr, PKN1-myr, PKN2-myr and PLK1-myr on *Pdk1*$^{lox/lox}$ cell line (A) Clonogenic assay of *Pdk1*$^{lox/lox}$;*LSL-Trp53*$^{R172H/+}$ cells expressing ITK-myr, MAP2K5-myr, PKN1-myr and PKN2-myr treated with EtOH and 4-OHT in comparison to empty vector (pWZL). A representative picture is shown, n = 3 replicates. (B) MTT assay of *Pdk1*$^{lox/lox}$;*LSL-Trp53*$^{R172H/+}$ cells expressing MAP2K5-myr, PKN1-myr, PKN2-myr and PLK1-myr treated with EtOH and 4-OHT in comparison to empty vector (pWZL). Data are shown as mean ± SD; n = 3 replicates. ***p < 0.001, **p < 0.01, *p < 0.05, ns p > 0.05, stepwise two-way ANOVA with Bonferroni correction (n=3). (C) qPCR

showing the expression of MAP2K5-myr, PKN1-myr, PKN2-myr and PLK1-myr in *Pdk1*$^{lox/lox}$*;LSL-Trp53*$^{R172H/+}$ cell line.

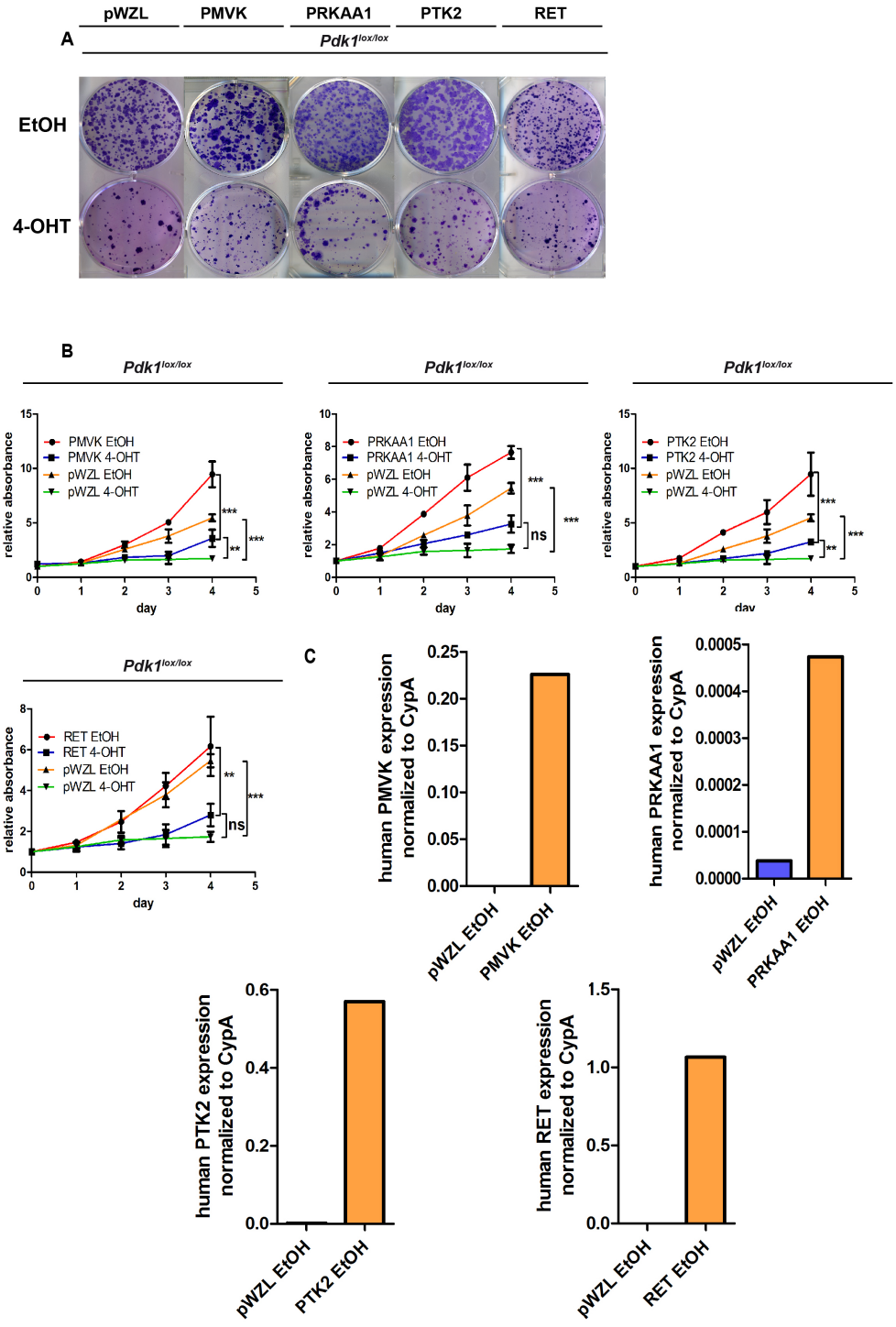

Figure 7-9: Expression of PMVK-myr, PRKAA1-myr, PTK2-myr and RET-myr on *Pdk1*$^{lox/lox}$ cell line
(A) Clonogenic assay of *Pdk1*$^{lox/lox}$*;LSL-Trp53*$^{R172H/+}$ cells expressing PMVK-myr, PRKAA1-myr, PTK2-myr and RET-myr treated with EtOH and 4-OHT in comparison to empty vector (pWZL). A representative picture is shown, n = 3 replicates. (B) MTT assay of *Pdk1*$^{lox/lox}$*;LSL-Trp53*$^{R172H/+}$ cells expressing PMVK-myr, PRKAA1-myr, PTK2-myr and RET-myr treated with EtOH and 4-OHT in comparison to empty vector (pWZL). Data are shown as mean ± SD; n = 3 replicates. ***p < 0.001, **p < 0.01, *p < 0.05, ns p > 0.05, stepwise two-way ANOVA with Bonferroni correction (n=3). (C) qPCR showing the expression of PMVK-myr, PRKAA1-myr, PTK2-myr and PLK1-myr in *Pdk1*$^{lox/lox}$*;LSL-Trp53*$^{R172H/+}$ cell line.

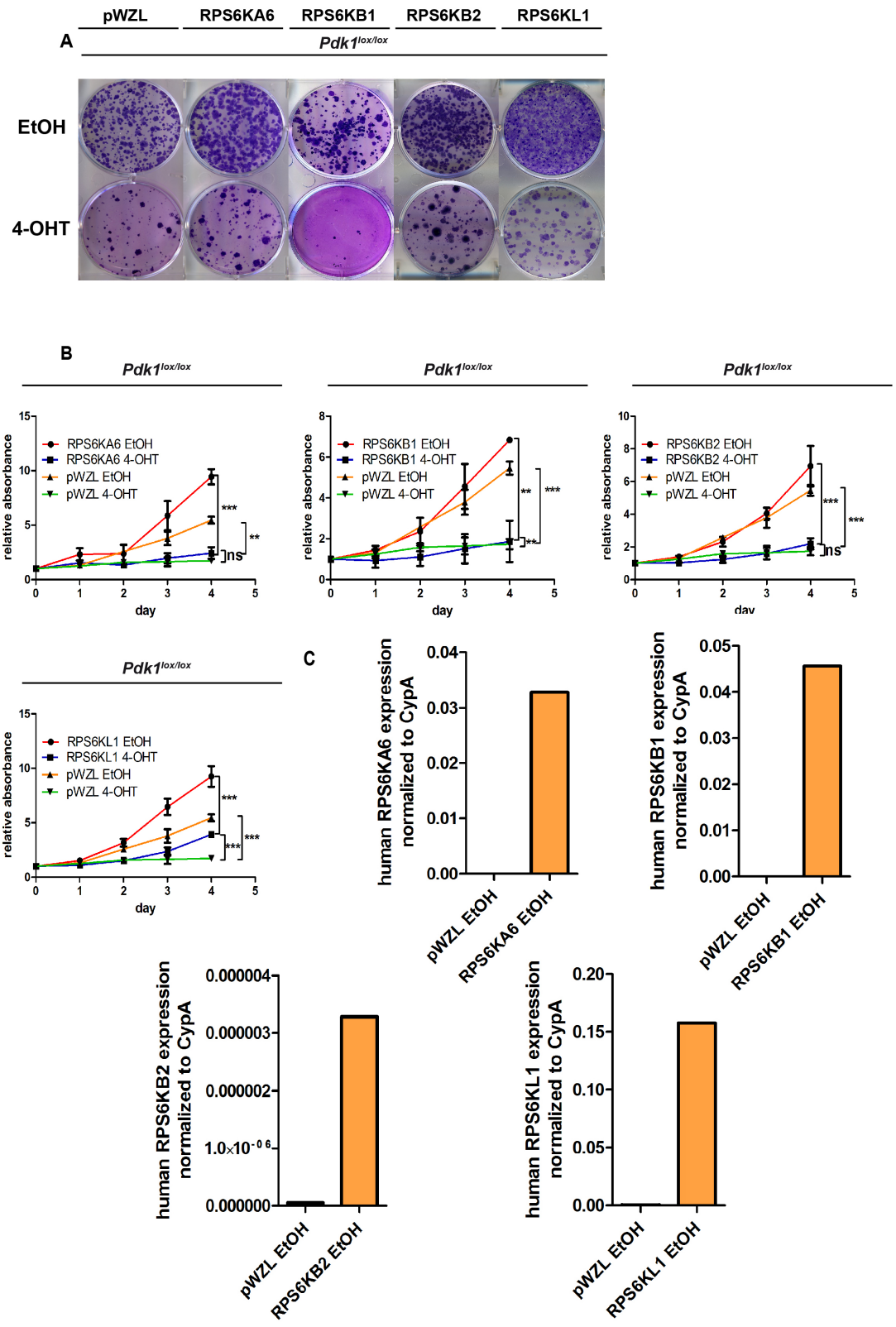

Figure 7-10: Expression of RPS6KA6-myr, RPS6KB1-myr, RPS6KB2-myr and RPS6KL1-myr on *Pdk1*$^{lox/lox}$ cell line A) Clonogenic assay of *Pdk1*$^{lox/lox}$;*LSL-Trp53*$^{R172H/+}$ cells expressing RPS6KA6-myr, RPS6KB1-myr, RPS6KB2-myr and RPS6KL1-myr treated with EtOH and 4-OHT in comparison to empty vector (pWZL). A representative picture is shown, n = 3 replicates. (B) MTT assay of *Pdk1*$^{lox/lox}$;*LSL-Trp53*$^{R172H/+}$ cells expressing RPS6KA6-myr, RPS6KB1-myr, RPS6KB2-myr and RPS6KL1-myr treated

with EtOH and 4-OHT in comparison to empty vector (pWZL). Data are shown as mean ± SD; n = 3 replicates. ***p < 0.001, **p < 0.01, *p < 0.05, ns p > 0.05, stepwise two-way ANOVA with Bonferroni correction (n=3). (C) qPCR showing the expression of RPS6KA6-myr, RPS6KB1-myr, RPS6KB2-myr and RPS6KL1-myr in *Pdk1*$^{lox/lox}$;*LSL-Trp53*$^{R172H/+}$ cell line.

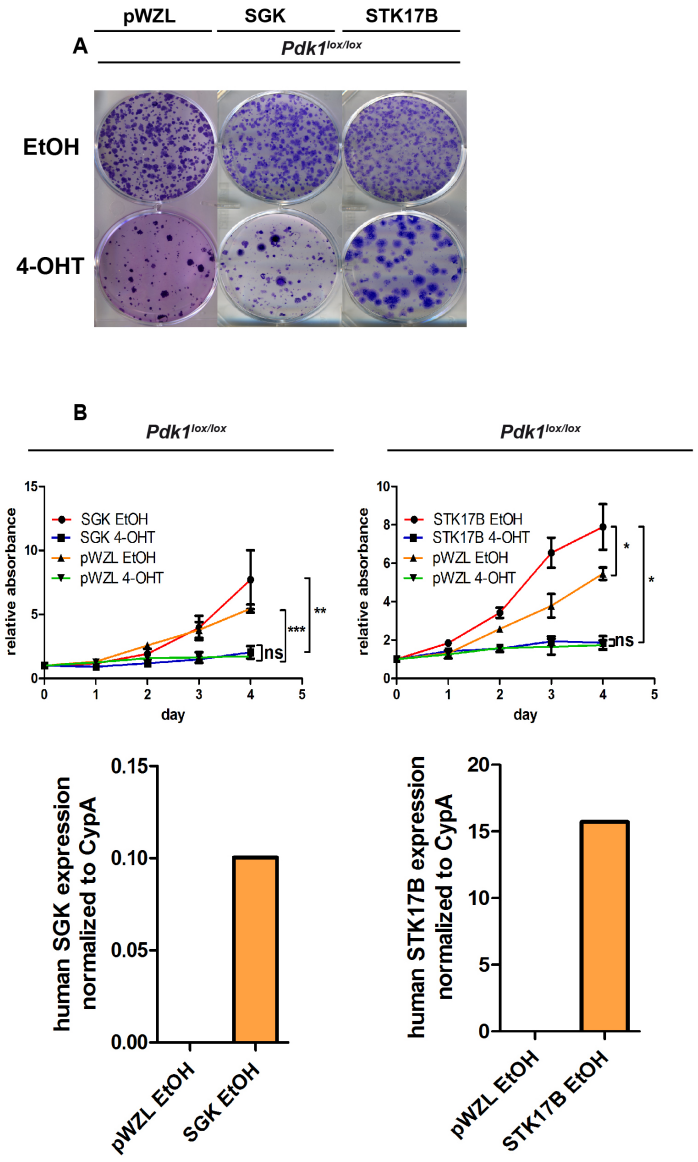

Figure 7-11: Expression of SGK-myr and STK17B-myr on *Pdk1*$^{lox/lox}$ cell line A) Clonogenic assay of *Pdk1*$^{lox/lox}$;*LSL-Trp53*$^{R172H/+}$ cells expressing SGK-myr and STK17B-myr treated with EtOH and 4-OHT in comparison to empty vector (pWZL). A representative picture is shown, n = 3 replicates. (B) MTT assay of *Pdk1*$^{lox/lox}$;*LSL-Trp53*$^{R172H/+}$ cells expressing SGK-myr and STK17B-myr treated with EtOH and 4-OHT in comparison to empty vector (pWZL). Data are shown as mean ± SD; n = 3 replicates. ***p < 0.001, **p < 0.01, *p < 0.05, ns p > 0.05, stepwise two-way ANOVA with Bonferroni correction (n=3). (C) qPCR showing the expression of SGK-myr and STK17B-myr in *Pdk1*$^{lox/lox}$;*LSL-Trp53*$^{R172H/+}$ cell line.

7.6. Human relevance of kinases used in this study

Witkiewicz et al. performed whole-exome sequencing on a total of 109 micro-dissected human PDAC cases and noticed substantial genetic heterogeneity in PDAC, comparable with other solid tumour entities. Here, the frequency of mutations, amplifications or deletions of the genes coding for the kinases expressed in this study is reported (Figure 7-14) (data using cbio portal).

CKS1B is amplified in 24% of the cases and *AKT1* was found to be amplified in 17% of the samples, thus indicating that our results could be relevant in human PDAC.

The overexpression of some kinases which are coded by genes that were often found to be amplified in this study (like *ADCK5*, *FASTK*, *PMVK*) did not show a functional effect upon Pdk1 loss. This means that they might be important for human PDAC but are not relevant for the development of Pdk1 resistance.

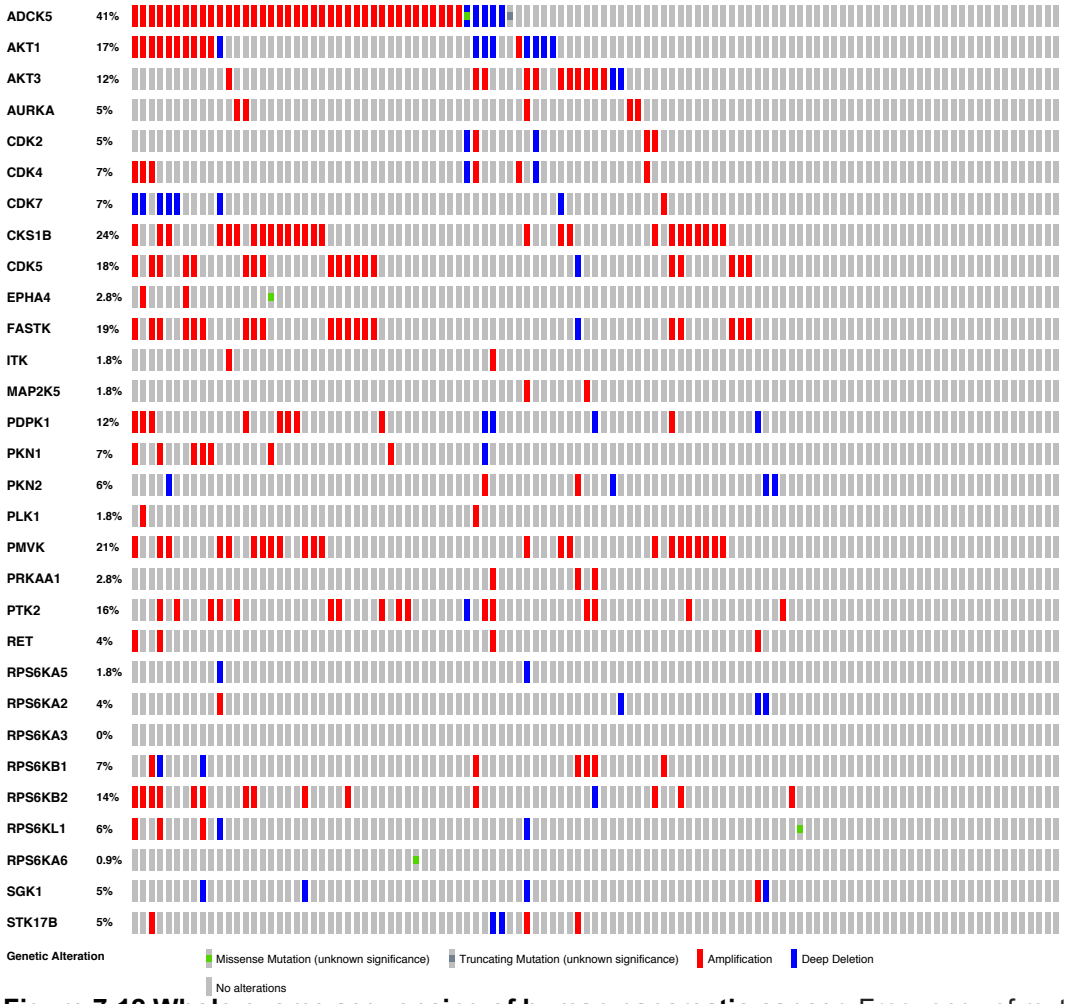

Figure 7-12 Whole-exome sequencing of human pancreatic cancer. Frequency of mutations, amplifications and deletions of genes coding for the kinases pertinent to the analyses in this thesis. The display was extracted from the whole-exome sequencing of human pancreatic cancer (Data from cbioportal; Witkiewicz et al., 2015). Amplification is shown in red; deletion in blue and missense mutation in green.

8. Discussion

Pdk1 is essential for the initiation and progression of *Kras*^{G12D} driven pancreatic tumour since its deletion prevents tumour formation, ADM and PI3K activation in the *Kras*^{G12D} model *in vitro* and *in vivo (*Eser et al., 2013*)*. It has been shown that phosphorylation of AKT-T308, GSK3β-S9 and RSK (p90RSK-T359/S363) was blocked when *Pdk1* was deleted in the *Kras*^{G12D} model (Eser et al., 2013), suggesting that these molecules are important effectors in PDAC carcinogenesis.

The main downstream pathways of PDK1 are known, but it is highly relevant to understand which ones are functionally responsible for tumour maintanance, in order to potentially use them as therapeutical targets.

8.1. Role of Akt1 in PDAC cell proliferation and metabolism

AKT is one of the main direct targets of PDK1. Among the different subtypes, AKT1 is the one mainly involved in growth and cell proliferation (Pearce et al., 2010).

As mentioned above, the phosphorylation of pAKT-T308 was blocked when *Pdk1* was deleted in the *Kras*^{G12D} model (Eser et al., 2013).

Moreover, functional ADM assays with the PI3K-inhibitor GDC 0941 on human acinar cells showed that ADM formation was reduced in a dose-dependent manner and that GDC 0941 inhibited AKT-T308 phosphorylation (Eser et al., 2013). This explains the importance of Pdk1 as well as the dependency of PI3K/Pdk1 signaling on Akt activation.

However, previous data showed that the inhibition of Pdk1 did not completely block activation of Akt (Hofler et al., 2011). This could be explained by an alternative mode of activation involving an AKT autophosphorylation and a phosphorylation of mTOR on multiple sites (Hofler et al., 2011). For example, it was lately shown that Mi375 targets Pdk1 in pancreatic carcinoma and suppresses cell growth by modulating the phosphorylation of the AKT signaling pathway (Zhou et al., 2014).

Consistent with previous data from our laboratory, we could show that a myristoylated form of Akt1 was able to completely rescue Pdk1 loss leading to a comparable proliferation pattern among *Pdk1*$^{lox/lox}$ cells treated with either EtOH or 4-OHT.

It is also remarkable that the rescue result was observed on Akt1, but not on Akt3, although this kinase was also found to be amplified in human whole genome sequencing data (Figure 7-12).

Among the analysed downstream pathways of Akt1, Gsk3β showed to be hyperactivated as well when Akt1-myr was expressed. Thus, this kinase could represent a further therapeutic target.
Furthermore, the importance of Kras and Pdk1 in glucose metabolism among pancreatic cancer cells has already been shown. For this reason, we performed functional metabolic assays, that demonstrated that glucose uptake was much higher in cells expressing Akt1 (80%) than in pWZL cells (50%).
Consistent with these data showing the importance of this kinase in the proliferation of pancreatic cancer cell lines, AKT1 was shown to be amplified or mutated in 17% of cases of sequenced human pancreatic cancer samples (Witkiewicz et al., 2015).
Because Akt1 showed to be the only one able to completely bypass Pdk1 loss, it probably plays a very important role in the carcinogenesis of pancreatic cancer and should be investigated as a possible therapeutical target.
Supporting our hypothesis, a recent study has shown that an Akt1 inhibitor inhibits human NSCLC cell growth more effectively than a pan-Akt inhibitor (Chorner and Moorehead, 2018).

8.2. The role of RSK members in PDAC

RSKs are directly regulated by the RAF/MEK/ERK signaling cascade, which represents an important effector pathway of Kras. The ribosomal protein S6 kinase family is involved in several kinds of tumours. It requires Pdk1 phosphorylation for its activation. Colorectal cancer (Slattery et al., 2011), breast cancer (Serra et al., 2013) and skin cancer (Skoudy et al., 2011) are often associated with members of RSK family.
Slattery and colleagues observed that genetic variations of some members of the RSK family are associated with higher risk of developing colorectal cancer and that they interact significantly with other genes operating in similar mechanisms, including Akt1, FRAP1, NFκB1, and *PIK3CA* (Slattery et al., 2011).
In this study, RPS6KA3 (RSK2), RPS6KA5, RPS6KA6 (RSK4), RPS6KB1 (p70s6k), RPS6KB2 and RPS6KL1 were analysed. A partial rescue of *Pdk1*-KO phenotype was obtained by expression of RPS6KA5-myr.

Previous experiments of our laboratory (C. Veltkamp, unpublished data) showed that Rsk2 could partially rescue Pdk1 loss. Previous studies have shown that RSK2 plays a key role in neoplastic transformation of human skin cells (Cho et al., 2012).

8.3. The role of CKS1B in PDAC cell lines

An association between CKS1B and pancreatic cancer is so far not known.
So far, its importance is known in other tumour entities like non-small-cell lung cancer (NSCLC), multiple myeloma and breast cancer progression. In multiple myeloma and breast cancer CKS1B activates MEK/ERK pathways and in multiple myeloma and NSCLC, STAT3 (Shi et al., 2010, Wang et al., 2009). Furthermore, Shi and colleagues showed that the overexpression of CKS1B in multiple myeloma cells induces drug-resistance and both studies reported that elevated expression is associated with a poor prognosis (Shi et al., 2010, Wang et al., 2009).
Moreover, Shi and colleagues demonstrated that CKS1B is essential for myeloma cell growth and survival by using gene knockdown. As a matter of fact, CKS1B-knockdown inhibited and CKS1B-overexpression activated STAT3 and MEK/ERK signaling pathways, demonstrating that STAT3 and MEK/ERK signaling pathways are the CKS1B downstream signaling pathways (Shi et al., 2010).
Wang and colleagues showed that Cks1 overexpression inhibited apoptosis of breast cancer cells via activation of the anti-apoptotic MEK/ERK signal pathway (Wang et al., 2009). Moreover, MEK/ERK pathway was activated by CKS1b since they showed that phosphorylated Erk was down-regulated in CKS1 shRNA cells.
Similarly to the previous results, showing a crucial role of CKSB in the development of other tumor entities, we suggest that CKS1B might also play an important role in the development of PDAC.
In fact we showed that the expression of CKS1B-myr leads to a substantial rescue of the Pdk1-KO phenotype in all the three lines, suggesting an alternative pathway to the classical PI3K/AKT one. Moreover, amplifications of CKS1B have been found in 24% of human pancreatic cancer cases by exome sequencing (Witkiewicz et al., 2015).
Further investigations like experiments *in vivo* should be performed in order to better understand its function and role in pancreatic cancer.

9. Conclusion

Pdk1 is essential for the mantainance of *Kras*^{G12D}-driven pancreatic tumour cell lines, since *Pdk1*-KO cells show a significantly decreased growth and a reduction in the metabolic activity.

Up to now, it has not been known which Pdk1-dependent signalling pathways are involved as well as how resistance mechanisms against Pi3k/Pdk1 inhibition develop. In this work I identified some kinases which are able to induce cell proliferation despite Pdk1 loss, leading to a complete or partial rescue of the cytostatic phenotype.

Therefore, a further step will be to express these kinases in "*in vivo*" models and try to establish possible therapeutical approaches based on them.

10. References

AICHLER, M., SEILER, C., TOST, M., SIVEKE, J., MAZUR, P. K., DA SILVA-BUTTKUS, P., BARTSCH, D. K., LANGER, P., CHIBLAK, S., DURR, A., HOFLER, H., KLOPPEL, G., MULLER-DECKER, K., BRIELMEIER, M. & ESPOSITO, I. 2012. Origin of pancreatic ductal adenocarcinoma from atypical flat lesions: a comparative study in transgenic mice and human tissues. *J Pathol,* 226**,** 723-34.

AMADOU, A., WADDINGTON ACHATZ, M. I. & HAINAUT, P. 2018. Revisiting tumor patterns and penetrance in germline TP53 mutation carriers: temporal phases of Li-Fraumeni syndrome. *Curr Opin Oncol,* 30**,** 23-29.

ASANO, T., YAO, Y., ZHU, J., LI, D., ABBRUZZESE, J. L. & REDDY, S. A. 2004. The PI 3-kinase/Akt signaling pathway is activated due to aberrant Pten expression and targets transcription factors NF-kappaB and c-Myc in pancreatic cancer cells. *Oncogene,* 23**,** 8571-80.

BARTHEL, A., OKINO, S. T., LIAO, J., NAKATANI, K., LI, J., WHITLOCK, J. P., JR. & ROTH, R. A. 1999. Regulation of GLUT1 gene transcription by the serine/threonine kinase Akt1. *J Biol Chem,* 274**,** 20281-6.

BERNDT, N., HAMILTON, A. D. & SEBTI, S. M. 2011. Targeting protein prenylation for cancer therapy. *Nat Rev Cancer,* 11**,** 775-91.

BOSETTI, C., LUCENTEFORTE, E., SILVERMAN, D. T., PETERSEN, G., BRACCI, P. M., JI, B. T., NEGRI, E., LI, D., RISCH, H. A., OLSON, S. H., GALLINGER, S., MILLER, A. B., BUENO-DE-MESQUITA, H. B., TALAMINI, R., POLESEL, J., GHADIRIAN, P., BAGHURST, P. A., ZATONSKI, W., FONTHAM, E., BAMLET, W. R., HOLLY, E. A., BERTUCCIO, P., GAO, Y. T., HASSAN, M., YU, H., KURTZ, R. C., COTTERCHIO, M., SU, J., MAISONNEUVE, P., DUELL, E. J., BOFFETTA, P. & LA VECCHIA, C. 2012. Cigarette smoking and pancreatic cancer: an analysis from the International Pancreatic Cancer Case-Control Consortium (Panc4). *Ann Oncol,* 23**,** 1880-8.

BRYANT, K. L., MANCIAS, J. D., KIMMELMAN, A. C. & DER, C. J. 2014. KRAS: feeding pancreatic cancer proliferation. *Trends Biochem Sci,* 39**,** 91-100.

CASTELLANO, E. & DOWNWARD, J. 2011. RAS Interaction with PI3K: More Than Just Another Effector Pathway. *Genes Cancer,* 2**,** 261-74.

CHO, Y. Y., LEE, M. H., LEE, C. J., YAO, K., LEE, H. S., BODE, A. M. & DONG, Z. 2012. RSK2 as a key regulator in human skin cancer. *Carcinogenesis,* 33**,** 2529-37.

CHORNER, P. M. & MOOREHEAD, R. A. 2018. A-674563, a putative AKT1 inhibitor that also suppresses CDK2 activity, inhibits human NSCLC cell growth more effectively than the pan-AKT inhibitor, MK-2206. *PLoS One,* 13**,** e0193344.

COLLINS, M. A., BEDNAR, F., ZHANG, Y., BRISSET, J. C., GALBAN, S., GALBAN, C. J., RAKSHIT, S., FLANNAGAN, K. S., ADSAY, N. V. & PASCA DI MAGLIANO, M. 2012a. Oncogenic Kras is required for both the initiation and maintenance of pancreatic cancer in mice. *J Clin Invest,* 122**,** 639-53.

COLLINS, M. A., BRISSET, J. C., ZHANG, Y., BEDNAR, F., PIERRE, J., HEIST, K. A., GALBAN, C. J., GALBAN, S. & DI MAGLIANO, M. P. 2012b. Metastatic pancreatic cancer is dependent on oncogenic Kras in mice. *PLoS One,* 7**,** e49707.

COLLISSON, E. A., TREJO, C. L., SILVA, J. M., GU, S., KORKOLA, J. E., HEISER, L. M., CHARLES, R. P., RABINOVICH, B. A., HANN, B., DANKORT, D.,

SPELLMAN, P. T., PHILLIPS, W. A., GRAY, J. W. & MCMAHON, M. 2012. A central role for RAF-->MEK-->ERK signaling in the genesis of pancreatic ductal adenocarcinoma. *Cancer Discov,* 2**,** 685-93.
DI MAGLIANO, M. P. & LOGSDON, C. D. 2013. Roles for KRAS in pancreatic tumor development and progression. *Gastroenterology,* 144**,** 1220-9.
DUCREUX, M., CUHNA, A. S., CARAMELLA, C., HOLLEBECQUE, A., BURTIN, P., GOERE, D., SEUFFERLEIN, T., HAUSTERMANS, K., VAN LAETHEM, J. L., CONROY, T., ARNOLD, D. & COMMITTEE, E. G. 2015. Cancer of the pancreas: ESMO Clinical Practice Guidelines for diagnosis, treatment and follow-up. *Ann Oncol,* 26 Suppl 5**,** v56-68.
ELSTROM, R. L., BAUER, D. E., BUZZAI, M., KARNAUSKAS, R., HARRIS, M. H., PLAS, D. R., ZHUANG, H., CINALLI, R. M., ALAVI, A., RUDIN, C. M. & THOMPSON, C. B. 2004. Akt stimulates aerobic glycolysis in cancer cells. *Cancer Res,* 64**,** 3892-9.
ESER, S., REIFF, N., MESSER, M., SEIDLER, B., GOTTSCHALK, K., DOBLER, M., HIEBER, M., ARBEITER, A., KLEIN, S., KONG, B., MICHALSKI, C. W., SCHLITTER, A. M., ESPOSITO, I., KIND, A. J., RAD, L., SCHNIEKE, A. E., BACCARINI, M., ALESSI, D. R., RAD, R., SCHMID, R. M., SCHNEIDER, G. & SAUR, D. 2013. Selective requirement of PI3K/PDK1 signaling for Kras oncogene-driven pancreatic cell plasticity and cancer. *Cancer Cell,* 23**,** 406-20.
ESER, S., SCHNIEKE, A., SCHNEIDER, G. & SAUR, D. 2014. Oncogenic KRAS signalling in pancreatic cancer. *Br J Cancer,* 111**,** 817-22.
GARGIULO, S., TORRINI, M., OLLILA, S., NASTI, S., PASTORINO, L., CUSANO, R., BONELLI, L., BATTISTUZZI, L., MASTRACCI, L., BRUNO, W., SAVARINO, V., SCIALLERO, S., BORGONOVO, G., NYSTROM, M., BIANCHI-SCARRA, G., MARENI, C. & GHIORZO, P. 2009. Germline MLH1 and MSH2 mutations in Italian pancreatic cancer patients with suspected Lynch syndrome. *Fam Cancer,* 8**,** 547-53.
GIARDIELLO, F. M., BRENSINGER, J. D., TERSMETTE, A. C., GOODMAN, S. N., PETERSEN, G. M., BOOKER, S. V., CRUZ-CORREA, M. & OFFERHAUS, J. A. 2000. Very high risk of cancer in familial Peutz-Jeghers syndrome. *Gastroenterology,* 119**,** 1447-53.
HIDALGO, M. 2010. Pancreatic cancer. *N Engl J Med,* 362**,** 1605-17.
HIRABAYASHI, M., INOUE, M., SAWADA, N., SAITO, E., ABE, S. K., HIDAKA, A., IWASAKI, M., YAMAJI, T., SHIMAZU, T. & TSUGANE, S. 2019. Helicobacter pylori infection, atrophic gastritis, and risk of pancreatic cancer: A population-based cohort study in a large Japanese population: the JPHC Study. *Sci Rep,* 9**,** 6099.
HOFLER, A., NICHOLS, T., GRANT, S., LINGARDO, L., ESPOSITO, E. A., GRIDLEY, S., MURPHY, S. T., KATH, J. C., CRONIN, C. N., KRAUS, M., ALTON, G., XIE, Z., SUTTON, S., GEHRING, M. & ERMOLIEFF, J. 2011. Study of the PDK1/AKT signaling pathway using selective PDK1 inhibitors, HCS, and enhanced biochemical assays. *Anal Biochem,* 414**,** 179-86.
HRUBAN, R. H., GOGGINS, M., PARSONS, J. & KERN, S. E. 2000. Progression model for pancreatic cancer. *Clin Cancer Res,* 6**,** 2969-72.
HRUBAN, R. H., MAITRA, A. & GOGGINS, M. 2008. Update on pancreatic intraepithelial neoplasia. *Int J Clin Exp Pathol,* 1**,** 306-16.
IQBAL, J., RAGONE, A., LUBINSKI, J., LYNCH, H. T., MOLLER, P., GHADIRIAN, P., FOULKES, W. D., ARMEL, S., EISEN, A., NEUHAUSEN, S. L., SENTER,

L., SINGER, C. F., AINSWORTH, P., KIM-SING, C., TUNG, N., FRIEDMAN, E., LLACUACHAQUI, M., PING, S., NAROD, S. A. & HEREDITARY BREAST CANCER STUDY, G. 2012. The incidence of pancreatic cancer in BRCA1 and BRCA2 mutation carriers. *Br J Cancer,* 107**,** 2005-9.

JENSEN, C. J., BUCH, M. B., KRAG, T. O., HEMMINGS, B. A., GAMMELTOFT, S. & FRODIN, M. 1999. 90-kDa ribosomal S6 kinase is phosphorylated and activated by 3-phosphoinositide-dependent protein kinase-1. *J Biol Chem,* 274**,** 27168-76.

KASTRINOS, F., MUKHERJEE, B., TAYOB, N., WANG, F., SPARR, J., RAYMOND, V. M., BANDIPALLIAM, P., STOFFEL, E. M., GRUBER, S. B. & SYNGAL, S. 2009. Risk of pancreatic cancer in families with Lynch syndrome. *JAMA,* 302**,** 1790-5.

KOHN, A. D., SUMMERS, S. A., BIRNBAUM, M. J. & ROTH, R. A. 1996. Expression of a constitutively active Akt Ser/Thr kinase in 3T3-L1 adipocytes stimulates glucose uptake and glucose transporter 4 translocation. *J Biol Chem,* 271**,** 31372-8.

LANGNER, C. 2017. [Hereditary gastric and pancreatic cancer]. *Pathologe,* 38**,** 164-169.

LEMKE, J., SCHAFER, D., SANDER, S., HENNE-BRUNS, D. & KORNMANN, M. 2014. Survival and prognostic factors in pancreatic and ampullary cancer. *Anticancer Res,* 34**,** 3011-20.

LOWENFELS, A. B. & MAISONNEUVE, P. 2004. Epidemiology and prevention of pancreatic cancer. *Jpn J Clin Oncol,* 34**,** 238-44.

LU, M., WAN, M., LEAVENS, K. F., CHU, Q., MONKS, B. R., FERNANDEZ, S., AHIMA, R. S., UEKI, K., KAHN, C. R. & BIRNBAUM, M. J. 2012. Insulin regulates liver metabolism in vivo in the absence of hepatic Akt and Foxo1. *Nat Med,* 18**,** 388-95.

MA, J. & JEMAL, A. 2013. The rise and fall of cancer mortality in the USA: why does pancreatic cancer not follow the trend? *Future Oncology,* 9**,** 917-919.

MAJUMDER, P. K. & SELLERS, W. R. 2005. Akt-regulated pathways in prostate cancer. *Oncogene,* 24**,** 7465-74.

MALVEZZI, M., BERTUCCIO, P., LEVI, F., LA VECCHIA, C. & NEGRI, E. 2014. European cancer mortality predictions for the year 2014. *Ann Oncol,* 25**,** 1650-6.

MATSUBAYASHI, H., TAKAORI, K., MORIZANE, C., MAGUCHI, H., MIZUMA, M., TAKAHASHI, H., WADA, K., HOSOI, H., YACHIDA, S., SUZUKI, M., USUI, R., FURUKAWA, T., FURUSE, J., SATO, T., UENO, M., KIYOZUMI, Y., HIJIOKA, S., MIZUNO, N., TERASHIMA, T., MIZUMOTO, M., KODAMA, Y., TORISHIMA, M., KAWAGUCHI, T., ASHIDA, R., KITANO, M., HANADA, K., FURUKAWA, M., KAWABE, K., MAJIMA, Y. & SHIMOSEGAWA, T. 2017. Familial pancreatic cancer: Concept, management and issues. *World J Gastroenterol,* 23**,** 935-948.

NOTTA, F., CHAN-SENG-YUE, M., LEMIRE, M., LI, Y., WILSON, G. W., CONNOR, A. A., DENROCHE, R. E., LIANG, S. B., BROWN, A. M., KIM, J. C., WANG, T., SIMPSON, J. T., BECK, T., BORGIDA, A., BUCHNER, N., CHADWICK, D., HAFEZI-BAKHTIARI, S., DICK, J. E., HEISLER, L., HOLLINGSWORTH, M. A., IBRAHIMOV, E., JANG, G. H., JOHNS, J., JORGENSEN, L. G., LAW, C., LUDKOVSKI, O., LUNGU, I., NG, K., PASTERNACK, D., PETERSEN, G. M., SHLUSH, L. I., TIMMS, L., TSAO, M. S., WILSON, J. M., YUNG, C. K., ZOGOPOULOS, G., BARTLETT, J. M., ALEXANDROV, L. B., REAL, F. X.,

CLEARY, S. P., ROEHRL, M. H., MCPHERSON, J. D., STEIN, L. D., HUDSON, T. J., CAMPBELL, P. J. & GALLINGER, S. 2016. A renewed model of pancreatic cancer evolution based on genomic rearrangement patterns. *Nature,* 538**,** 378-382.

ONO, H., SHIMANO, H., KATAGIRI, H., YAHAGI, N., SAKODA, H., ONISHI, Y., ANAI, M., OGIHARA, T., FUJISHIRO, M., VIANA, A. Y., FUKUSHIMA, Y., ABE, M., SHOJIMA, N., KIKUCHI, M., YAMADA, N., OKA, Y. & ASANO, T. 2003. Hepatic Akt activation induces marked hypoglycemia, hepatomegaly, and hypertriglyceridemia with sterol regulatory element binding protein involvement. *Diabetes,* 52**,** 2905-13.

PEARCE, L. R., KOMANDER, D. & ALESSI, D. R. 2010. The nuts and bolts of AGC protein kinases. *Nat Rev Mol Cell Biol,* 11**,** 9-22.

PFAFFL, M. W. 2001. A new mathematical model for relative quantification in real-time RT-PCR. *Nucleic Acids Res,* 29**,** e45.

PINHO, A. V., ROOMAN, I., REICHERT, M., DE MEDTS, N., BOUWENS, L., RUSTGI, A. K. & REAL, F. X. 2011. Adult pancreatic acinar cells dedifferentiate to an embryonic progenitor phenotype with concomitant activation of a senescence programme that is present in chronic pancreatitis. *Gut,* 60**,** 958-66.

PYLAYEVA-GUPTA, Y., GRABOCKA, E. & BAR-SAGI, D. 2011. RAS oncogenes: weaving a tumorigenic web. *Nat Rev Cancer,* 11**,** 761-74.

REBOURS, V., BOUTRON-RUAULT, M. C., SCHNEE, M., FEREC, C., MAIRE, F., HAMMEL, P., RUSZNIEWSKI, P. & LEVY, P. 2008. Risk of pancreatic adenocarcinoma in patients with hereditary pancreatitis: a national exhaustive series. *Am J Gastroenterol,* 103**,** 111-9.

RISHI, A., GOGGINS, M., WOOD, L. D. & HRUBAN, R. H. 2015. Pathological and molecular evaluation of pancreatic neoplasms. *Semin Oncol,* 42**,** 28-39.

ROBERTS, N. J., JIAO, Y., YU, J., KOPELOVICH, L., PETERSEN, G. M., BONDY, M. L., GALLINGER, S., SCHWARTZ, A. G., SYNGAL, S., COTE, M. L., AXILBUND, J., SCHULICK, R., ALI, S. Z., ESHLEMAN, J. R., VELCULESCU, V. E., GOGGINS, M., VOGELSTEIN, B., PAPADOPOULOS, N., HRUBAN, R. H., KINZLER, K. W. & KLEIN, A. P. 2012. ATM mutations in patients with hereditary pancreatic cancer. *Cancer Discov,* 2**,** 41-6.

SCHEFFZEK, K., AHMADIAN, M. R., KABSCH, W., WIESMULLER, L., LAUTWEIN, A., SCHMITZ, F. & WITTINGHOFER, A. 1997. The Ras-RasGAP complex: structural basis for GTPase activation and its loss in oncogenic Ras mutants. *Science,* 277**,** 333-8.

SCHNEIDER, G., SAUR, D. & SCHMID, R. M. 2007. Pancreatic cancer — Molecular alterations. *The Chinese-German Journal of Clinical Oncology,* 6**,** 102–106.

SCHONHUBER, N., SEIDLER, B., SCHUCK, K., VELTKAMP, C., SCHACHTLER, C., ZUKOWSKA, M., ESER, S., FEYERABEND, T. B., PAUL, M. C., ESER, P., KLEIN, S., LOWY, A. M., BANERJEE, R., YANG, F., LEE, C. L., MODING, E. J., KIRSCH, D. G., SCHEIDELER, A., ALESSI, D. R., VARELA, I., BRADLEY, A., KIND, A., SCHNIEKE, A. E., RODEWALD, H. R., RAD, R., SCHMID, R. M., SCHNEIDER, G. & SAUR, D. 2014. A next-generation dual-recombinase system for time- and host-specific targeting of pancreatic cancer. *Nat Med,* 20**,** 1340-1347.

SERRA, V., EICHHORN, P. J., GARCIA-GARCIA, C., IBRAHIM, Y. H., PRUDKIN, L., SANCHEZ, G., RODRIGUEZ, O., ANTON, P., PARRA, J. L., MARLOW, S., SCALTRITI, M., PEREZ-GARCIA, J., PRAT, A., ARRIBAS, J., HAHN, W. C.,

KIM, S. Y. & BASELGA, J. 2013. RSK3/4 mediate resistance to PI3K pathway inhibitors in breast cancer. *J Clin Invest,* 123**,** 2551-63.
SHI, L., WANG, S., ZANGARI, M., XU, H., CAO, T. M., XU, C., WU, Y., XIAO, F., LIU, Y., YANG, Y., SALAMA, M., LI, G., TRICOT, G. & ZHAN, F. 2010. Over-expression of CKS1B activates both MEK/ERK and JAK/STAT3 signaling pathways and promotes myeloma cell drug-resistance. *Oncotarget,* 1**,** 22-33.
SKOUDY, A., HERNANDEZ-MUNOZ, I. & NAVARRO, P. 2011. Pancreatic ductal adenocarcinoma and transcription factors: role of c-Myc. *J Gastrointest Cancer,* 42**,** 76-84.
SLATTERY, M. L., LUNDGREEN, A., HERRICK, J. S. & WOLFF, R. K. 2011. Genetic variation in RPS6KA1, RPS6KA2, RPS6KB1, RPS6KB2, and PDK1 and risk of colon or rectal cancer. *Mutat Res,* 706**,** 13-20.
WANG, X. C., TIAN, J., TIAN, L. L., WU, H. L., MENG, A. M., MA, T. H., XIAO, J., XIAO, X. L. & LI, C. H. 2009. Role of Cks1 amplification and overexpression in breast cancer. *Biochem Biophys Res Commun,* 379**,** 1107-13.
WANG, Y., LI, G., GOODE, J., PAZ, J. C., OUYANG, K., SCREATON, R., FISCHER, W. H., CHEN, J., TABAS, I. & MONTMINY, M. 2012. Inositol-1,4,5-trisphosphate receptor regulates hepatic gluconeogenesis in fasting and diabetes. *Nature,* 485**,** 128-32.
WIEMAN, H. L., WOFFORD, J. A. & RATHMELL, J. C. 2007. Cytokine stimulation promotes glucose uptake via phosphatidylinositol-3 kinase/Akt regulation of Glut1 activity and trafficking. *Mol Biol Cell,* 18**,** 1437-46.
WITKIEWICZ, A. K., MCMILLAN, E. A., BALAJI, U., BAEK, G., LIN, W. C., MANSOUR, J., MOLLAEE, M., WAGNER, K. U., KODURU, P., YOPP, A., CHOTI, M. A., YEO, C. J., MCCUE, P., WHITE, M. A. & KNUDSEN, E. S. 2015. Whole-exome sequencing of pancreatic cancer defines genetic diversity and therapeutic targets. *Nat Commun,* 6**,** 6744.
WU, X., RENUSE, S., SAHASRABUDDHE, N. A., ZAHARI, M. S., CHAERKADY, R., KIM, M. S., NIRUJOGI, R. S., MOHSENI, M., KUMAR, P., RAJU, R., ZHONG, J., YANG, J., NEISWINGER, J., JEONG, J. S., NEWMAN, R., POWERS, M. A., SOMANI, B. L., GABRIELSON, E., SUKUMAR, S., STEARNS, V., QIAN, J., ZHU, H., VOGELSTEIN, B., PARK, B. H. & PANDEY, A. 2014. Activation of diverse signalling pathways by oncogenic PIK3CA mutations. *Nat Commun,* 5**,** 4961.
YOON, S. & SEGER, R. 2006. The extracellular signal-regulated kinase: multiple substrates regulate diverse cellular functions. *Growth Factors,* 24**,** 21-44.
ZHOU, J., SONG, S., HE, S., ZHU, X., ZHANG, Y., YI, B., ZHANG, B., QIN, G. & LI, D. 2014. MicroRNA-375 targets PDK1 in pancreatic carcinoma and suppresses cell growth through the Akt signaling pathway. *Int J Mol Med,* 33**,** 950-6.